Out-of-sequence, basement-involved structures in the Sadlerochit Mountains region of the Arctic National Wildlife Refuge, Alaska: Evidence and implications from fission-track thermochronology

Paul B. O'Sullivan[†]
Department of Earth Sciences, Syracuse University, Syracuse, New York 13244, USA

Wesley K. Wallace[‡]
Geophysical Institute and *Department of Geology and Geophysics, University of Alaska, Fairbanks, Alaska 99775, USA*

ABSTRACT

Fission-track thermochronology and structural analysis set limits on the timing and nature of structural development of the Sadlerochit Mountains, along the southern edge of the coastal plain in the Arctic National Wildlife Refuge (ANWR) of northeastern Alaska. The Sadlerochit Mountains are the northernmost part of the north-vergent Brooks Range fold-and-thrust belt and lie close to the Arctic continental margin. Thermochronology results indicate that sedimentary rocks exposed within Ignek Valley, south of the Sadlerochit Mountains, were subjected to two episodes of rapid cooling from elevated paleotemperatures at ca. 45 Ma and at some time since ca. 31 Ma, whereas similar-aged rocks exposed along the northern flank of the Sadlerochit Mountains cooled rapidly at ca. 45 Ma and ca. 27 Ma. Combined with five additional analyses from the Beli Unit #1 well, located northwest of the Sadlerochit Mountains, the thermochronology results indicate that the Sadlerochit Mountains region was progressively heated during Late Cretaceous through middle Eocene time, after which two major episodes of rapid cooling occurred in the middle Eocene at ca. 45 ± 3 Ma (±2σ) and in the late Oligocene at ca. 27 ± 2 Ma (±2σ).

These episodes of rapid cooling are interpreted to have occurred in response to kilometer-scale erosional denudation resulting from rapid (≤5 m.y.) uplift due to structural thickening during the emplacement of thrust sheets in a basement-involved duplex. Initially, at least one thrust sheet was probably emplaced to the north of the Sadlerochit Mountains at ca. 45 Ma. Subsequently, at ca. 27 Ma, (1) the Sadlerochit Mountains thrust sheet was probably emplaced out of sequence behind the earlier-emplaced thrust sheet(s), and (2) basement-involved deformation formed structures beneath the coastal plain to the north. Both of these events occurred far within the continent, >1200 km from the southern Alaska convergent plate boundary.

These results indicate that maximum burial, and hence peak hydrocarbon generation, occurred prior to middle Eocene time, before the formation of potential traps in and immediately north of the Sadlerochit Mountains. However, (1) hydrocarbons generated from these rocks could have migrated updip into existing stratigraphic traps prior to structural deformation, and (2) hydrocarbons generated later in more distal parts of the basin could have migrated updip into subsurface structures formed in middle Eocene and late Oligocene time north of the Sadlerochit Mountains and along strike to the east and west.

Keywords: Alaska, Arctic National Wildlife Refuge (ANWR), basement-involved thrusting, Brooks Range, fission-track dating, out-of-sequence thrusting, Sadlerochit Mountains, thermotectonics.

INTRODUCTION

The Brooks Range of northern Alaska (Fig. 1)—the northernmost part of the North American Cordillera—lies ~1200 km landward of the present convergent boundary between North America and the Pacific plate. Although the Brooks Range had its origins in the Mesozoic, fission-track thermochronology has revealed that much of the topography of the range resulted from Cenozoic deformation (e.g., O'Sullivan et al., 1993, 1997, 1998a, 1998b; Blythe et al., 1996). The northeastern Brooks Range is a prominent northward salient that likely formed entirely during the Cenozoic (Kelley and Foland, 1987; Wallace and Hanks, 1990; O'Sullivan, 1993, 1994; O'Sullivan et al., 1993, 1998b; Hanks et al., 1994). The Sadlerochit Mountains are the northernmost part of this salient and lie only 35 km south of the Arctic Ocean.

Relatively little detailed information has been published on the character and evolution of structures in the Sadlerochit Mountains. This information includes mainly geologic maps (Reiser et al., 1970, 1971; Bader and Bird, 1986; Robinson et al., 1989) and reconnaissance structural studies (Kelley and Foland, 1987; Leiggi, 1987; Mull, 1987; Wallace and Hanks, 1990; Wallace, 1993; Cole et al., 1999), although one detailed study has been done in the important northeastern salient of the Sadlerochit Mountains (Meigs, 1989).

Limits on the absolute timing of structures in and around the Sadlerochit Mountains also are lacking, owing primarily to the absence of exposed syn- to posttectonic deposits that could be used to date the

[†]Present address: Apatite to Zircon, Inc., 1075 Matson Road, Viola, Idaho 87872, USA; e-mail: osullivan@apatite.com.
[‡]E-mail: wallace@gi.alaska.edu.

GSA Bulletin; November 2002; v. 114; no. 11; p. 1356–1378; 14 figures; 2 tables.

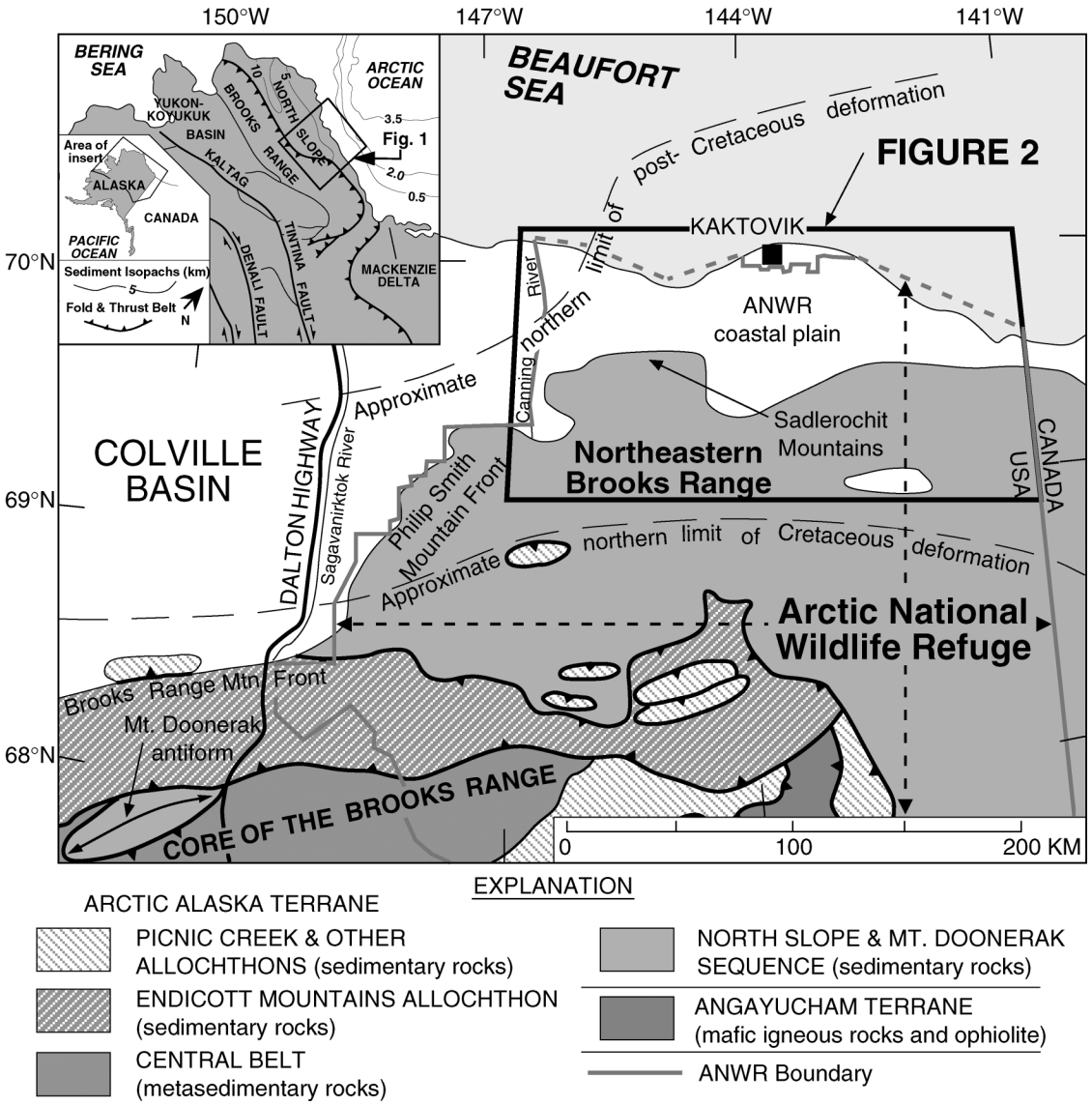

Figure 1. Generalized geologic map of northeastern Alaska, showing the location of the Arctic National Wildlife Refuge (ANWR), the northeastern Brooks Range, and other features specifically mentioned in the text.

activity of structures. Subsurface data from the Arctic National Wildlife Refuge (ANWR) coastal plain, or ''1002 area,'' are limited to a regional grid of two-dimensional seismic reflection lines, run in 1984 and 1985, and a single well (Chevron KIC #1 near Kaktovik), the results of which remain confidential. The U.S. Geological Survey has conducted two major assessments of the petroleum potential of the 1002 area (Bird and Magoon, 1987; ANWR Assessment Team, 1999), in which the determination of the ages of structures throughout the region was based primarily on interpretation of the limited seismic reflection data. It is important to note that the ANWR Assessment Team's (1999) evaluation (Cole et al., 1999; Moore, 1999; Potter et al., 1999; Rowan, 1999) also made limited use of preliminary apatite fission-track thermochronology results by O'Sullivan (1993) and O'Sullivan et al. (1993), who suggested that the Sadlerochit Mountains had possibly undergone two episodes of denudation during the middle to late Cenozoic. However, these preliminary results relied largely on rocks exposed ~20–30 km to the east along a structural trend at Sabbath Creek (Fig. 2), so O'Sullivan (1993) and O'Sullivan et al. (1993) were not able to relate distinct denudation events to the formation of specific structures within either the mountains or the coastal plain to the north.

This paper presents apatite and zircon fission-track thermochronology data from the Sadlerochit Mountains vicinity that document multiple periods of deformation during the Cenozoic, despite the location of the range far within the continent. The data also support the interpretation that (1) Cenozoic deformation involved depositional basement at a position near the leading edge of the fold-and-thrust belt, and (2) the basement-involved structures are not simply progressively younger toward the foreland, reflecting a forward-propagating sequence, but instead resulted from out-of-sequence activity behind the deformation front (Boyer and Elliot, 1982; Butler, 1987; Morley, 1988). Such out-of-sequence deformation is a predictable element of the evo-

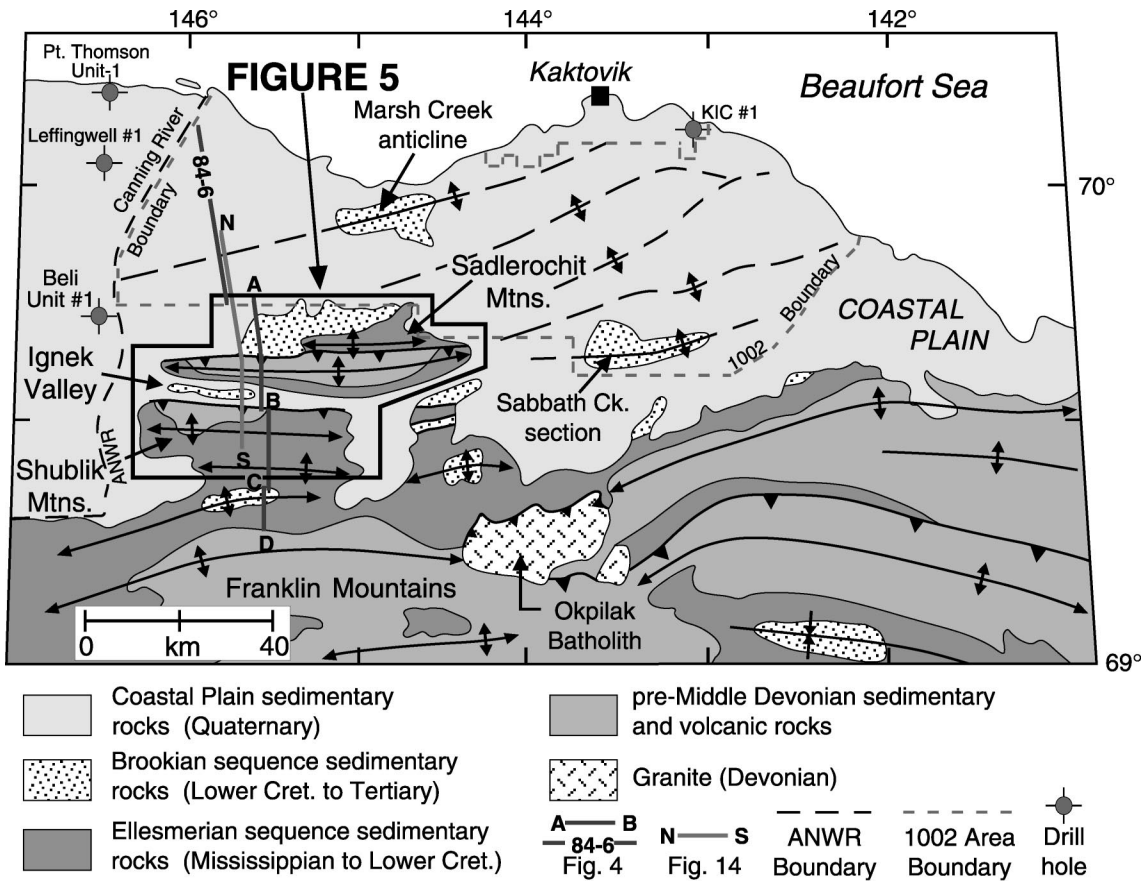

Figure 2. Tectonic map of the northeastern Brooks Range, showing the location of the Sadlerochit and Shublik mountain ranges, Ignek Valley, the Beli Unit #1 well, seismic line 84-6, and other features mentioned in the text. Map modified from Wallace and Hanks (1990).

lution of an orogenic wedge as it deforms internally to maintain critical taper (e.g., Dahlen, 1990; Hardy et al., 1998). However, out-of-sequence structures can be difficult to identify in nature, especially where the absence of syn- to postdeformational rocks precludes direct determination of the relative age of structures. The results from the Sadlerochit Mountains provide an excellent example of how fission-track thermochronology can provide tight limits on both the absolute age and structural evolution of fold-and-thrust belts.

The fission-track results also are relevant to an important political and economic question, the petroleum potential of the coastal plain of ANWR (Figs. 1, 2). This area is commonly considered to be North America's most promising area for future onshore petroleum exploration, but whether to open the coastal plain, or 1002 area, to petroleum exploration is a subject of intense debate. The fission-track results and structural interpretations presented here provide some insights into the timing of petroleum maturation and migration relative to formation of potential trapping structures.

GEOLOGIC SETTING

The Sadlerochit Mountains are the northernmost range in the northeastern Brooks Range, separated by <35 km (22 miles) of coastal plain from the Beaufort Sea (Figs. 1, 2). The northeastern Brooks Range itself is a prominent arcuate northward salient at the eastern end of the east-trending main axis of the Brooks Range. The early evolution of the main axis of the Brooks Range involved significant shortening during initial emplacement of multiple allochthons in Middle Jurassic to Early Cretaceous time (e.g., Mull, 1982; Moore et al., 1994a). This deformation was followed by a period of later, lesser shortening that formed most of the present-day topographic relief of the Brooks Range and culminated with formation of the present range-front and foothills structures in Paleocene time (e.g., O'Sullivan, 1993, 1996; Moore et al., 1994a; O'Sullivan et al., 1997, 1998a). The northeastern Brooks Range (Fig. 1) formed as deformation continued northward from the eastern end of the main axis of the Brooks Range from Eocene to present (Kelley and Foland, 1987; Wallace and Hanks, 1990; O'Sullivan, 1993, 1994; O'Sullivan et al., 1993, 1998b; Hanks et al., 1994).

The stratigraphy of the region can be divided into three sequences that reflect major phases in the geologic evolution of the region (e.g., Bird and Molenaar, 1987) (Fig. 3). Depositional basement consists of a complex of penetratively deformed low-grade metasedimentary and subordinate metavolcanic rocks of pre–middle Devonian age. These are overlain with angular unconformity by the Ellesmerian sequence, a Mississippian to Lower Cretaceous succession of clastic and carbonate rocks deposited on a south-facing passive continental margin. The Mississippian Kekiktuk Conglomerate forms the base of the sequence and is separated by the Mississippian Kayak Shale from the carbonates of the Mississippian and Pennsylvanian Lisburne Group, which are exposed extensively throughout the northeastern Brooks Range. The Lis-

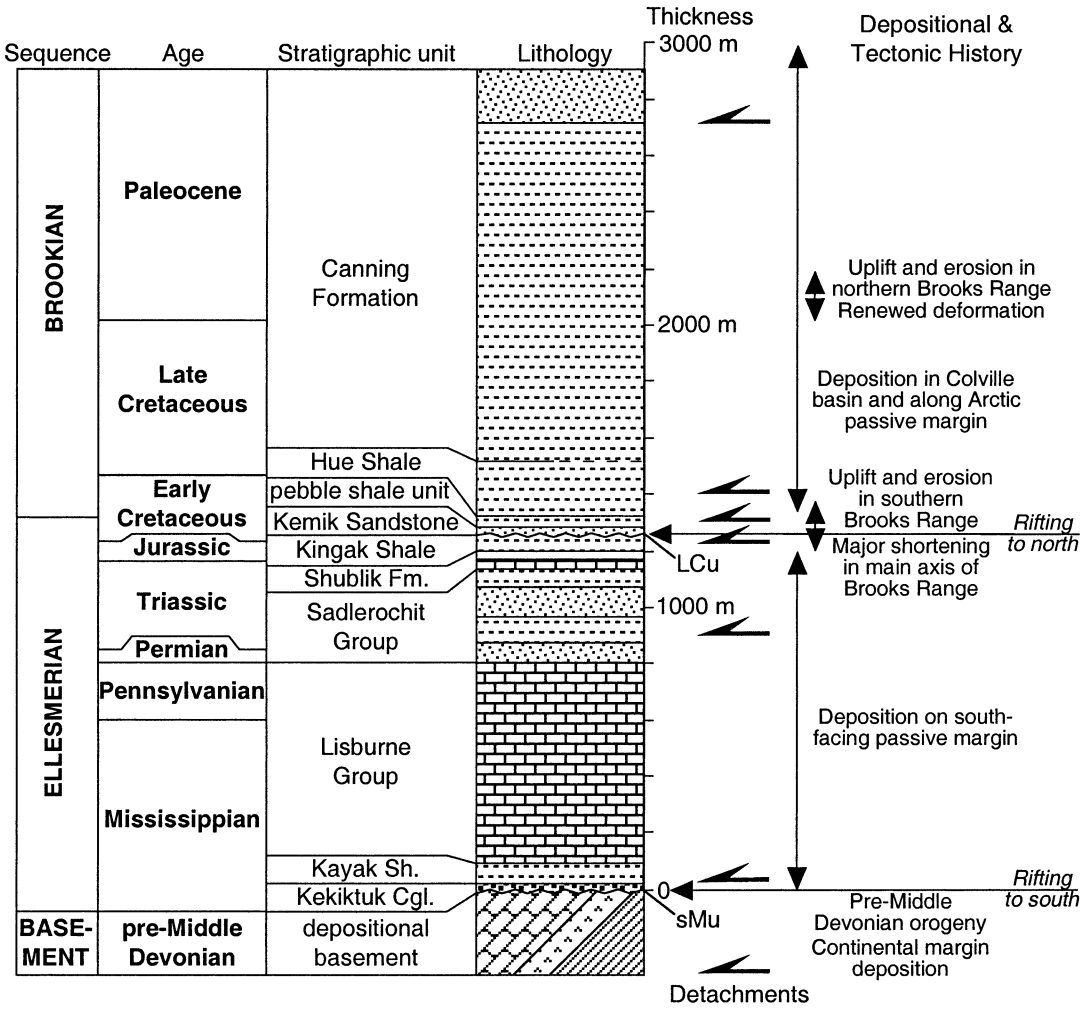

Figure 3. Generalized stratigraphic column for the Sadlerochit Mountains vicinity, showing significant structural detachments. Thicknesses are based principally on interpretation of data from Beli Unit #1 and Canning River Unit A-1 and B-1 wells (Plate 1 of Bird and Molenaar, 1987), but thicknesses display significant variation throughout the area. Kayak Shale and Kekiktuk Conglomerate pinch out depositionally to north in Sadlerochit Mountains, and the Lower Cretaceous unconformity (Lower Cretaceous unconformity) cuts progressively down section to north from northeastern Sadlerochit Mountains. The other unconformity is the sMu—sub-Mississippian unconformity.

burne Group is disconformably overlain by a succession of dominantly clastic units, including the Permian and Lower Triassic Sadlerochit Group, the Upper Triassic Shublik Formation, the Jurassic and Lower Cretaceous Kingak Shale, and the Lower Cretaceous Kemik Sandstone and pebble-shale unit. A major regional unconformity, the Lower Cretaceous unconformity, is exposed in the northeastern Sadlerochit Mountains at the base of the Kemik Sandstone. Erosion beneath the unconformity has cut down into the Sadlerochit Group there, but is thought to cut down into the basement in the subsurface to the northeast on the basis of seismic data and the regional pattern that is effectively documented by well and seismic data to the northwest (e.g., Bird and Molenaar, 1987; Bruns et al., 1987; Kelley and Foland, 1987; Potter et al., 1999; Grow et al., 1999). The Ellesmerian sequence is conformably overlain by the Brookian sequence, a succession that was derived by erosion from the Brooks Range and deposited to the north. This succession includes the Cretaceous Hue Shale, the Upper Cretaceous to Eocene Canning Formation, and the Eocene and younger Sagavanirktok Formation. These clastic units define a broadly coarsening-upward succession that represents northward progradation of the deposits as they progressively filled the basin.

The stratigraphy of the region has played a fundamental role in the character of structures formed in the northeastern Brooks Range (Kelley and Foland, 1987; Wallace and Hanks, 1990; Wallace, 1993; Cole et al., 1999) (Fig. 3). The largest structures in the northeastern Brooks Range are anticlinoria cored by basement rocks (Fig. 2). These anticlinoria are interpreted to represent large fault-bend folds in fault-bounded thrust sheets, or horses, in a duplex thrust system with a floor thrust at depth in basement and a roof thrust in the Kayak Shale (Fig. 4). The Kekiktuk Conglomerate deforms along with the basement below the roof thrust. The anticlinoria are smaller north of the Franklin Mountains, including those in the Sadlerochit Mountains, and probably reflect smaller horses in the duplex. Throughout most of the northeastern Brooks Range, the Lisburne and Sadlerochit Groups are deformed into symmetrical detachment folds above the Kayak Shale.

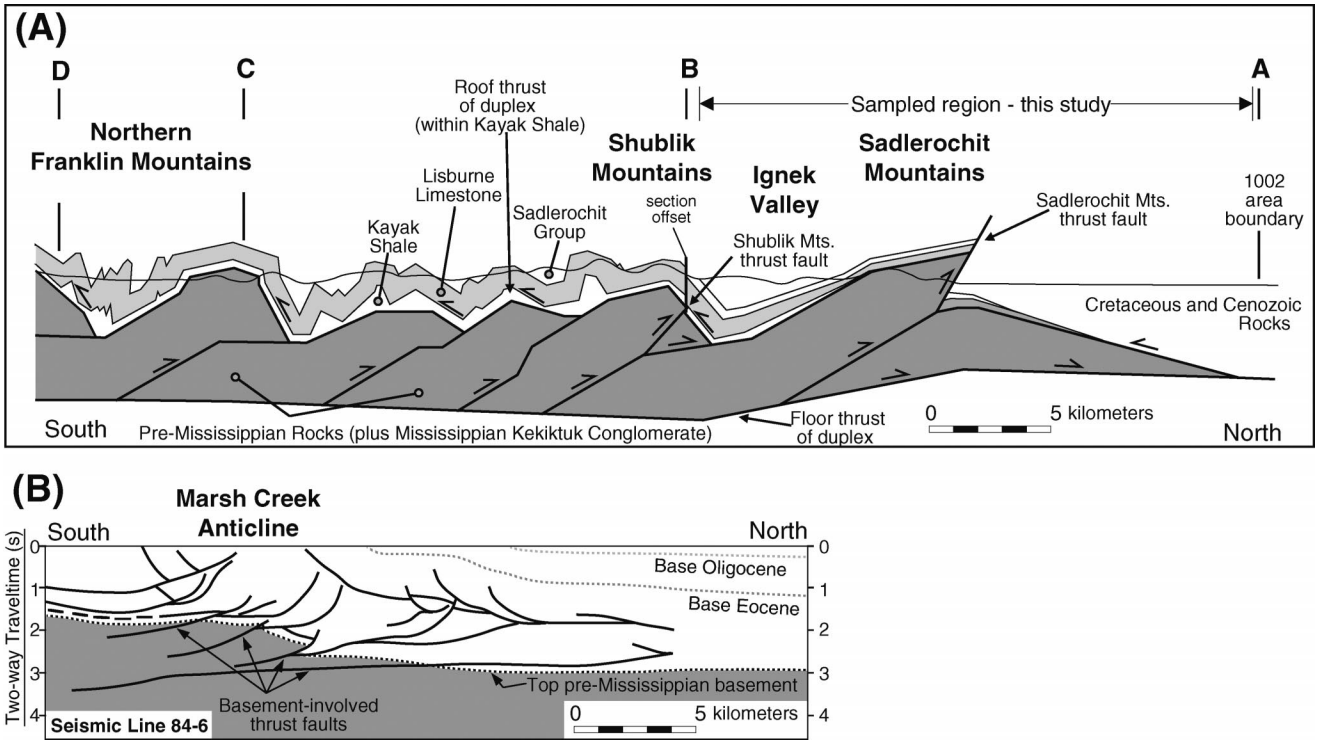

Figure 4. Presentation of known structures recognized within the Sadlerochit Mountains region. (A) Balanced cross section through the northern part of northeastern Brooks Range (modified from Wallace, 1993). Each basement-cored anticlinorium is interpreted to mark a horse in a duplex formed above a detachment at depth in basement (dark shading). The roof thrust in Kayak Shale terminates to north in the Sadlerochit Mountains owing to depositional discontinuity. All structures shown are interpreted to be Cenozoic in age. (B) Reproduced interpretation of seismic line 84-6 by Potter et al. (1999, plate BD2), indicating that basement rocks were involved in deformation beneath the coastal plain to the north of the Sadlerochit Mountains (at same scale as A).

Thrust faults that branch upward from or cut across the Kayak detachment are rare. Rocks younger than the Sadlerochit Group are eroded throughout most of the northeastern Brooks Range, but some of the best exposures of the Shublik through Canning Formations are found along the north flank of the Sadlerochit Mountains and along their south flank in Ignek Valley (e.g., Bird and Molenaar, 1987; Mull, 1987). The exposures here indicate that the structures in these rocks are bounded by a series of structural detachments, including detachments in the lower part of the Sadlerochit Group, the Kingak Shale, the pebble-shale unit, the Hue Shale, and the Canning Formation (Fig. 3). The relatively small stratigraphic thickness that separates these detachments means that the folds and faults formed between them are significantly smaller than the structures lower in the section.

The Sadlerochit and Shublik Mountains display some structural characteristics that differ from most of the rest of the northeastern Brooks Range (e.g., Kelley and Foland, 1987; Robinson et al., 1989; Wallace and Hanks, 1990; Wallace, 1993; Cole et al., 1999). First, a prominent thrust fault along the northern edge of each range places basement over rocks as young as the Canning Formation (Fig. 5). Although they did not form in crystalline basement, these range-front structures are similar to those found in the Laramide basement uplifts of the Rocky Mountains (e.g., Erslev, 1986; Mitra and Mount, 1998). The thrust in the Shublik Mountains defines the front of the entire range, and the thrust in the Sadlerochit Mountains defines the western range front, but a northeastern salient of the Sadlerochit Mountains lies to the north of the eastern end of the thrust. These faults appear to reflect thrust breakthrough of the leading edge of a fault-bend-folded basement horse (Mull, 1987; Meigs, 1989; Wallace and Hanks, 1990; Rogers, 1992; Wallace, 1993). The thrusts have cut up section across the normal position of the duplex roof thrust, perhaps as fault-propagation folds, and have left behind wedges of basement in the footwall (Fig. 4A). These anomalous thrusts probably are the result of a combination of two local stratigraphic differences, an unusually thick and competent carbonate section in the basement of the Sadlerochit and Shublik Mountains, and the northward depositional discontinuity in the Sadlerochit Mountains of the Kayak Shale, which normally serves as the roof thrust for the basement duplex. The discontinuity of the Kayak Shale also has resulted in an absence of detachment folds in the Sadlerochit Mountains, where the Lisburne and Sadlerochit have instead deformed along with basement (Fig. 4A). In the northeastern Sadlerochit Mountains, the Lower Cretaceous unconformity has cut down to the Sadlerochit Group and probably cuts down into basement in the subsurface to the north, leading to the absence of the Ellesmerian sequence in most subsurface structures of this area, although it may be preserved locally in paleo–structural lows (e.g., Bruns et al., 1987; Kelley and Foland, 1987; Cole et al., 1999; Grow et al., 1999; Potter et al., 1999).

A structural style similar to that observed in the northeastern Brooks Range is interpreted to continue northward into the subsurface of the coastal plain (Fig. 4B; Bruns et al., 1987; Kelley and Foland, 1987; Cole et al., 1999; Grow et al., 1999; Moore, 1999; Potter et al., 1999).

The limited seismic reflection data available show that the depth to the top of basement increases gradually northward toward the deformation front. Depth to basement is >5 km (16,000 feet) near the deformation front north of the Sadlerochit Mountains (Cole et al., 1999). Local relief on the top of basement and the geometry of underlying reflectors are interpreted to mark horses within the basement duplex (Fig. 4B). The geometry of the mostly Brookian strata above the basement is interpreted to define thin-skinned structures, including triangle zones.

Formation of the northeastern Brooks Range apparently postdates formation of the main east-west axis of the Brooks Range and occurred entirely during the Cenozoic (Kelley and Foland, 1987; Wallace and Hanks, 1990; O'Sullivan, 1993, 1994; O'Sullivan et al., 1993, 1998b; Hanks et al., 1994). Much of the topography of the northern part of the main axis of the Brooks Range formed at ca. 60 Ma, including formation of the range front and deformation of the foreland-basin deposits in the foothills to the north (O'Sullivan, 1996; O'Sullivan et al., 1997, 1998a; Blythe et al., 1996). Subsequently, deformation continued northward throughout the Cenozoic to form the northeastern Brooks Range. Fission-track thermochronology indicates that this deformation involved multiple episodes of rapid cooling, at ca. 45 Ma, ca. 35 Ma, and ca. 27 Ma, that are interpreted to represent periods of uplift and erosional unroofing in response to structural thickening (O'Sullivan, 1993, 1994; O'Sullivan et al., 1993, 1998a, 1998b; Hanks et al., 1994). A Cenozoic age of deformation is supported by involvement of rocks as young as Eocene (Canning Formation) in structures near the mountain front (e.g., Robinson et al., 1989) and involvement of rocks as young as Miocene and Pliocene in structures on the coastal plain, on the basis of surface and subsurface data (e.g., Reiser et al., 1970, 1971; Bruns et al., 1987; Kelley and Foland, 1987; Potter et al., 1999). Previous work (e.g., Bruns et al., 1987; Kelley and Foland, 1987; Dixon and Dietrich 1990; McMillen and O'Sullivan, 1992) has interpreted that a significant angular unconformity in the subsurface of the coastal plain indicates a middle Eocene deformational event and that the unconformity has itself been involved in later deformation. However, Potter et al. (1999) later questioned the existence of this middle Eocene unconformity and the deformational event that caused it. Seismicity and surficial deformation indicate that at least some deformation continues to the present beneath the coastal plain and offshore (Fig. 4B; e.g., Carter et al., 1986; Grantz et al., 1987).

EXPERIMENTAL PROCEDURES

Apatite Fission-Track Thermochronology (AFTT)

Apatite fission-track thermochronology (AFTT) provides a record of the thermal history of the host rock below temperatures of ~110 °C, which makes this technique ideal for testing models of denudation in response to deformation and uplift of upper-crustal rocks (e.g., Naeser, 1979; Gleadow et al., 1986). When fission tracks form in apatite, they have a fairly constant mean length of ~16 μm (Gleadow et al., 1986). Following their formation, fission tracks in apatite progressively shorten (anneal) at a rate that depends primarily on temperature (Gleadow et al., 1986; Green et al., 1989), which has led to the concept of a partial annealing zone (PAZ) to describe the temperature zone (~60–110 °C) in which fission tracks in apatite undergo accelerated annealing (e.g., Fitzgerald and Gleadow, 1988). Increased annealing results in shorter tracks, reduced track density, and a reduction in the fission-track age, whereas total annealing results in the reduction of the fission-track age to zero. Because new tracks continuously form throughout geologic time, the track-length distribution of the confined tracks in apatite grains directly reflects the sample's thermal history (Gleadow et al., 1986; Green et al., 1989).

It has been recognized that the annealing behavior of fission tracks in apatite is sensitive to chemical composition and that chlorine-rich apatites are more resistant to track annealing than fluorine-rich apatites (Green et al., 1985; Carlson et al., 1999; Donelick et al., 1999; Ketcham et al., 1999). This property suggests that the closure temperature for individual grains within a sample may vary significantly in response to variations in chlorine content. At temperatures below ~50–60 °C, fission tracks in common apatite anneal, but at a slow enough rate that little reduction in the AFTT age occurs, whereas at temperatures of ~110 °C or more, tracks anneal rapidly to result in total resetting of the AFTT age. Therefore, the depth to the top and base of the PAZ will depend on the chemical composition of the apatites, as well as on the geothermal gradient and on the duration of heating.

Zircon Fission-Track Thermochronology (ZFTT)

Zircon fission-track thermochronology (ZFTT) is useful for determining a sample's higher-temperature thermal history. Tagami et al. (1990) proposed that, as with apatite, a continuous temperature range exists within which spontaneous tracks in zircon reduce in length prior to totally annealing (a PAZ for zircon), with exposure to temperatures within the zircon PAZ resulting in a reduction in the ZFTT age. Incorporating the results from Tagami et al. (1990), Brandon et al. (1998) have suggested that the boundaries of the zircon PAZ range between ~180 and 280 °C, depending on the duration of the thermal event (their Fig. 6, p. 993). They also have suggested a range in the zircon closure temperature ~225–260 °C for rates of cooling between 1 and 100 °C/m.y., respectively. On the basis of these reports, we assume that ZFTT ages could potentially be totally reset at temperatures as low as ~225 °C, but the apparent ages would be significantly reduced owing to extended exposure to temperatures as low as ~180 °C.

Integration of Fission-Track and Vitrinite Reflectance Data

Although vitrinite reflectance (R_o) data do not provide limits on the age of maximum paleotemperatures, R_o values may be used as an indicator of maximum paleotemperature. All estimates of maximum paleotemperatures from R_o data presented here were determined by using the model proposed by Burnham and Sweeney (1989; their equation 2). After maximum paleotemperatures are estimated from fission-track and R_o data for samples from a vertical profile (e.g., a subsurface well sequence), a paleogeothermal gradient at the time of maximum paleotemperatures can be estimated from a maximum paleotemperature profile produced by plotting these values relative to depth. In a vertical section that has been hotter in the past, the paleogeothermal gradient can be compared with the present-day geothermal gradient to interpret the cause of the high paleotemperatures and the subsequent cooling to present temperatures. If one assumes that cooling has occurred because of removal of overburden by erosion, the amount of section removed can be estimated by dividing the amount of cooling (derived by subtracting the mean annual surface temperature at the time the section began to cool from the maximum paleotemperature to which rocks now at the surface were previously exposed) by the geothermal gradient. In many cases, including northern Alaska, it is important to know exactly when the sampled vertical sequence began to cool, as a significant decrease in mean annual surface temperature during the late Miocene

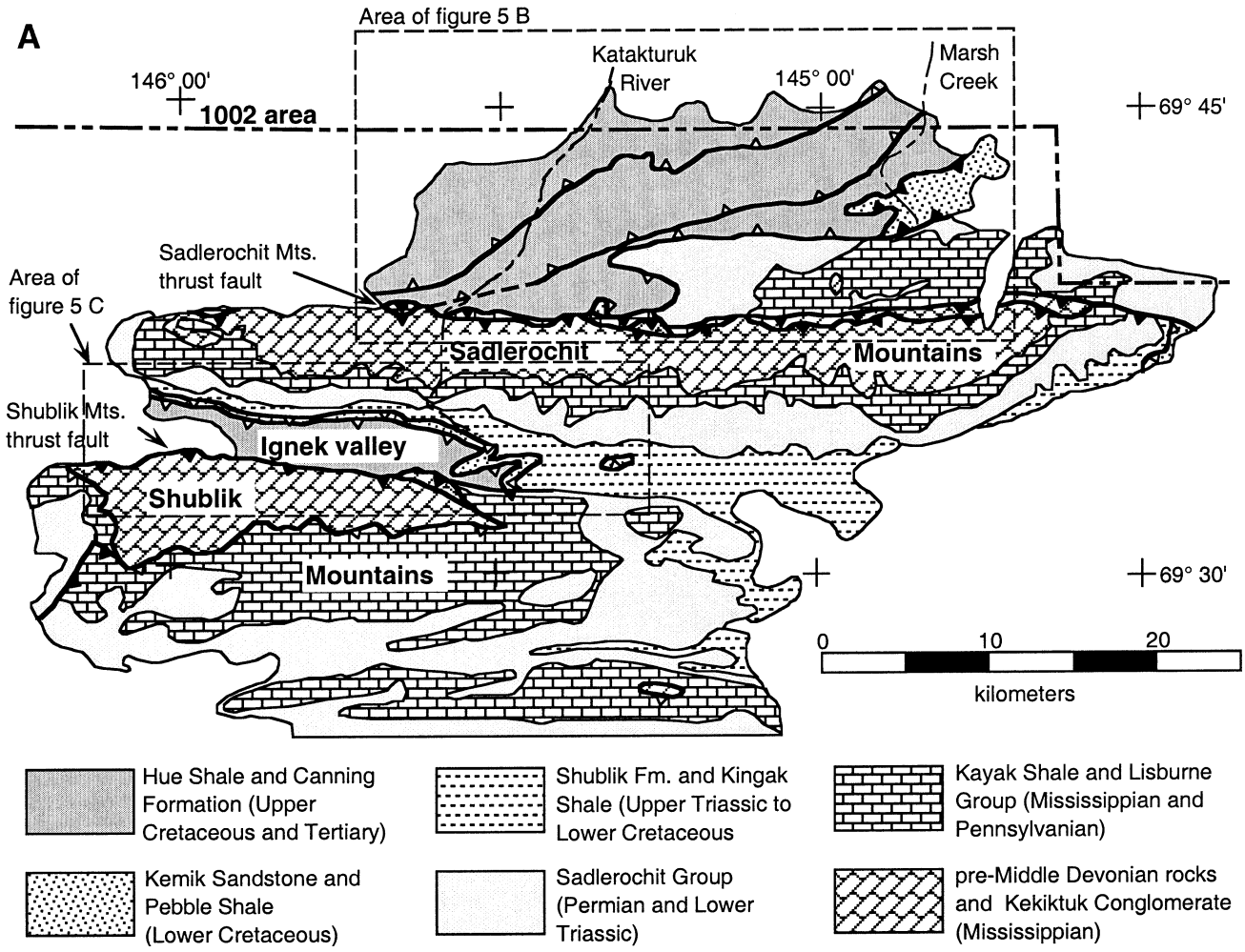

Figure 5. (A) Generalized geologic map of the Sadlerochit and Shublik Mountains (modified from Bader and Bird, 1987, based on data from Kelley and Foland, 1987; Robinson et al., 1989; Wallace and Hanks, 1990; Wallace, 1993; and field observations). Solid teeth on thrust faults indicate older-over-younger thrust faults that duplicate stratigraphic section; open teeth indicate younger-over-older structural detachment surfaces across which there has been no disruption of the normal stratigraphic succession. Maps of (B) northern Sadlerochit Mountains and of (C) Ignek valley show locations of fission-track and vitrinite reflectance samples collected for this study, as well as regional vitrinite reflectance values from Magoon et al. (1987). The apatite and zircon fission-track data are shown by sample location for each area. For each sample, the fission-track age, mean track length, standard deviation, and number of confined tracks measured are shown. Errors are ±1σ. Details are discussed in the text.

to Pliocene has resulted in noticeable subsurface cooling (O'Sullivan and Brown, 1998; O'Sullivan 1999).

Methodology

Nineteen ~2 kg samples were collected from sedimentary rocks exposed along two south-north transects on the northern flank of the east-trending Sadlerochit Mountains and from scattered outcrops within the Ignek Valley, to the south of the range (Fig. 5). To the east, the ''Marsh Creek transect'' follows Marsh Creek north from the northeastern front of the Sadlerochit Mountains. To the west, the ''Katakturuk River transect'' extends northward from the western front of the range along a small drainage west of the Katakturuk River. The Ignek Valley samples are from locations that span the width of the major syncline that defines the valley. The sampling areas were chosen specifically to determine the timing of deformation and consequent denudation related to different detachments and the structures formed above them (Fig. 5). Table 1 presents sample information, including locations and stratigraphic ages.

Five additional ~0.5 kg samples were obtained from sedimentary rocks within the Beli Unit #1 well located ~15 km to the northwest of the Sadlerochit Mountains on the west side of the Canning River (Fig. 2). The Beli Unit #1 well was chosen specifically for analysis because it was drilled over a basement-controlled structural high along strike with the northeastern salient of the Sadlerochit Mountains. Therefore, determining when cooling occurred within the well could potentially provide an independent check on the cooling history determined within that salient along the Marsh Creek transect.

All samples were processed, data on age and length of confined tracks were generated, and interpretations made according to the pro-

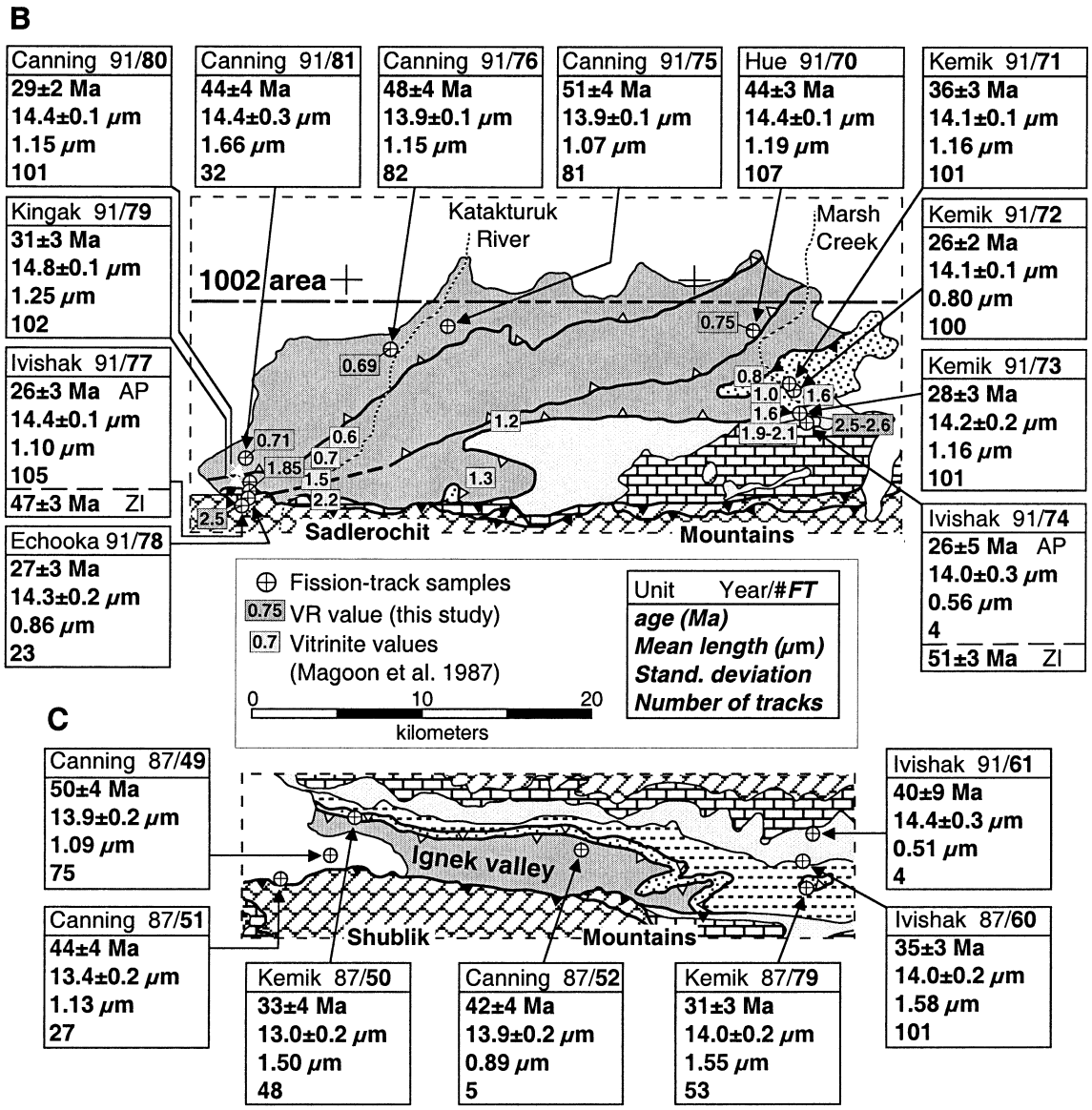

Figure 5. (*Continued.*)

cedures discussed previously in O'Sullivan (1996). Following microprobe analysis of >300 apatite grains from a number of the samples, we concluded that close to 100% of the apatite for which fission-track data were generated represented F-rich grains with <0.4 wt% Cl. The AFTT data generated for this study have therefore been interpreted by using the apatite system response (Laslett et al., 1987) based on an empirical kinetic description of laboratory annealing data in the Durango apatite standard with ~0.4 wt% Cl. In cases such as this study in which the analyzed apatite grains contain Cl in similar amounts as in Durango apatite, the Laslett et al. (1987) model gives predictions that are consistent with geologic constraints on annealing behavior (Green et al., 1989). However, as the apatite grains from the Sadlerochit Mountains samples contain slightly less Cl than Durango apatite, the paleotemperatures estimated by applying this model in this study are interpreted to be maximum values.

FISSION-TRACK RESULTS AND INTERPRETATIONS

The fission-track analytical results are presented in Table 2. With two exceptions, samples 93–1 and 93–2 from the Canning Formation in the Beli Unit #1 well, the AFTT ages were significantly younger than depositional ages, indicating that the samples were exposed to elevated paleotemperatures following deposition.

Figure 6 shows microprobe results for the 90 grains dated from two pairs of samples yielding significantly different AFTT ages from the same stratigraphic unit at different localities, including samples 71 and 72 from the Kemik Sandstone along Marsh Creek and samples 80 and 81 from the Canning Formation exposed along the Katakturuk River transect. These results indicate that all the grains dated in these four samples were F rich (<0.4 wt% Cl), and therefore the differences in AFTT ages can only be explained by different cooling histories.

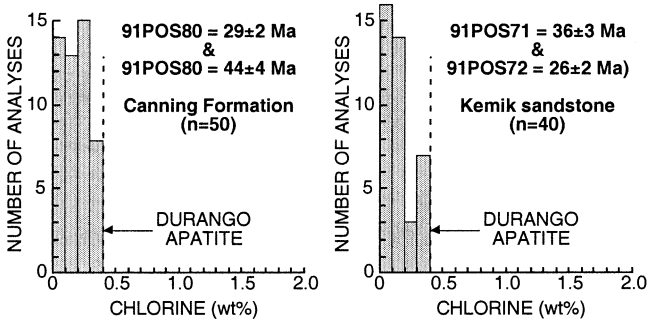

Figure 6. Summary histograms of the Cl contents in apatite grains dated in four representative samples from the Kemik Sandstone and the Canning Formation. Details are discussed in the text.

Apatite Fission-Track Samples from Ignek Valley

Samples from Ignek Valley, south of the Sadlerochit Mountains, yielded AFTT ages of 50 ± 4 to 31 ± 3 Ma (uncertainties are ±1σ unless otherwise stated) and mean confined-track lengths of 14.4 ± 0.3 to 13.0 ± 0.2 μm (Fig. 5, Table 2). A relationship seems to exist between a sample's stratigraphic position and its AFTT age (Fig. 7). For instance, samples from the Canning Formation at the top of the stratigraphic sequence have apatite ages of ca. 50–42 Ma and typically contain narrow distributions of mean confined-track lengths with standard deviations of <1.2 μm (Figs. 7, 8). However, down section, the AFTT ages decrease to ca. 31 Ma, and the mean track-length distributions broaden with standard deviations of >1.5 μm. The samples are distributed over a distance of ~30 km along strike, so local differences in thermal history could also have some influence on the distribution of ages.

Interpretation of the AFTT data from Ignek Valley suggests that the AFTT ages of the samples were totally reset following deposition owing to exposure to elevated paleotemperatures of >110 °C. Furthermore, for samples collected from the Canning Formation to have preserved their long mean lengths and narrow distributions, application of the track-annealing model of Laslett et al. (1987) indicates that these rocks must have (1) cooled rapidly (in <5 m.y.) from the proposed maximum paleotemperatures of >110 °C to paleotemperatures of ≤50 °C at the time suggested by the AFTT age (ca. 45 Ma), and (2) subsequently remained at temperatures of ~<50 °C. Modeling the AFTT data from the samples from deeper stratigraphic units suggests that they also were rapidly cooled from paleotemperatures of >110 °C at ca. 45 Ma. However, these rocks must have subsequently remained at elevated paleotemperatures of >60 °C for a period of time prior to later cooling to surface conditions. The youngest AFTT age of ca. 31 Ma determined from the partially reset samples represents a maximum for the timing of this later cooling.

Apatite Fission-Track Samples from the North Flank of the Sadlerochit Mountains

Samples from the north flank of the Sadlerochit Mountains yielded AFTT ages of 51 ± 3 to 26 ± 2 Ma and mean confined-track lengths of 14.8 ± 0.1 to 13.9 ± 0.1 μm (Table 2). Once again, a relationship exists between sample stratigraphic position and AFTT age (Fig. 7), although any geologic interpretation of the fission-track results must

TABLE 1. SAMPLE DETAILS FOR THE SADLEROCHIT MOUNTAINS AND IGNEK VALLEY REGION

Sample number	Latitude (N)	Longitude (W)	Elevation/depth (m)/(ft)	Formation	Stratigraphic subdivision	Proposed maximum temp.† (°C)	Estimated denudation‡ (km)
Outcrop—Ignek Valley							
87POS49	69°34.4′	146°00.3′	(482)/(1580)	Canning	Campanian–Paleocene	110–120	3.8–4.1
87POS50	69°35.3′	146°01.2′	(389)/(1275)	Kemik	Late Neocomian	120–135	4.1–4.6
87POS51	69°33.6′	146°05.2′	(335)/(1100)	Canning	Campanian–Paleocene	110–120	3.8–4.1
87POS52	69°34.0′	145°48.5′	(555)/(1820)	Canning	Campanian–Paleocene	110–120	3.8–4.1
88POS60	69°34.0′	145°20.1′	(805)/(2640)	Ivishak	Early–Middle Triassic	120–135	4.1–4.6
88POS79	69°33.4′	145°20.0′	(1034)/(3390)	Kemik	Late Neocomian	120–135	4.1–4.6
91POS61	69°34.9′	145°20.3′	(1311)/(4261)	Ivishak	Early–Middle Triassic	120–135	4.1–4.6
Outcrop—Front range of Sadlerochit Mountains							
91POS70	69°43.2′	144°54.3′	(451)/(1466)	Hue	Late Cretaceous	120–135	4.1–4.6
91POS71	69°41.9′	144°51.8′	(549)/(1784)	Kemik	Late Neocomian	160–180	5.5–6.3
91POS72	69°41.6′	144°51.3′	(549)/(1784)	Kemik	Late Neocomian	160–180	5.5–6.3
91POS73	69°40.7′	144°51.0′	(538)/(1750)	Kemik	Late Neocomian	160–180	5.5–6.3
91POS74	69°40.7′	144°50.9′	(534)/(1736)	Ivishak	Early–Middle Triassic	>200	>7.0
91POS75	69°43.5′	145°20.5′	(274)/(891)	Canning	Campanian–Paleocene	100–110	3.4–3.8
91POS76	69°42.9′	145°26.0′	(274)/(891)	Canning	Campanian–Paleocene	100–110	3.4–3.8
91POS77	69°38.3′	145°39.3′	(555)/(1820)	Ivishak	Early–Middle Triassic	>200	>7.0
91POS78	69°38.2′	145°39.0′	(470)/(1540)	Echooka	Permian	>200	>7.0
91POS79	69°38.9′	145°38.9′	(454)/(1489)	Kingak	Jurassic	120–135	4.1–4.6
91POS80	69°39.0′	145°38.9′	(427)/(1400)	Canning	Campanian–Paleocene	110–120	3.8–4.1
91POS81	69°39.5′	145°38.8′	(421)/(1380)	Canning	Campanian–Paleocene	110–120	3.8–4.1
Beli Unit #1 Well							
93-1	69°42.9′	146°32.2′	(–1005)/(–3266)	Sagavanirktok	Late Cretaceous–Miocene	75–85	1.3–1.5
93-2	69°42.9′	146°32.2′	(–1850)/(–6012)	Sagavanirktok	Late Cretaceous–Miocene	85–100	1.3–1.5
93-3	69°42.9′	146°32.2′	(–2620)/(–8515)	Canning	Campanian–Paleocene	110–125	1.3–1.5
93-4	69°42.9′	146°32.2′	(–3180)/(–10,335)	Hue	Late Cretaceous	115–130	1.3–1.5
93-5	69°42.9′	146°32.2′	(–3630)/(–11,798)	Ivishak	Early–Middle Triassic	135–155	1.3–1.5

†Maximum temperature values based on vitrinite values from the region (Magoon et al., 1987) converted to estimated maximum paleotemperatures by using the conversion of Burnham and Sweeney (1989, equation 2).

‡Estimated amounts of denudation for surface samples calculated by dividing the proposed maximum temperatures by the regional maximum paleogeothermal gradient of ~28 °C/km derived from the Beli Unit #1 and assuming a mean annual surface temperature of ~5 °C at the time of cooling. These estimates represent minimum values.

TABLE 2. ANALYTICAL RESULTS: SADLEROCHIT MOUNTAINS/IGNEK VALLEY REGION

Sample number (Unit)†	Type (Ap/Zi)	Number of grains	Standard track density ($\times 10^6$ cm^{-2})	Fossil track density ($\times 10^5$ cm^{-2})	Induced track density ($\times 10^6$ cm^{-2})	Chi square probability (%)	Fission-track age (Ma)	Uranium (ppm)	Mean track length (μm)	Standard deviation (μm)
Outcrop—Ignek Valley										
87POS49	Ap	25	2.548	2.302	2.066	38.5	49.9 ± 4.3	10.6	13.88 ± 0.18	1.09
TKc			(5734)	(156)	(1400)				(75)	
87POS50	Ap	25	2.548	2.140	2.872	76.1	33.4 ± 3.7	14.8	12.95 ± 0.22	1.50
Kk			(5734)	(89)	(1194)				(48)	
87POS51	Ap	20	2.548	3.274	3.338	74.6	43.9 ± 4.2	17.2	13.35 ± 0.22	1.13
TKc			(5734)	(127)	(1295)				(27)	
87POS52	Ap	21	2.548	2.865	3.063	84.5	41.9 ± 4.3	15.7	13.89 ± 0.48	0.89
TKc			(5734)	(107)	(1144)				(5)	
88POS60	Ap	25	2.548	5.284	6.810	76.6	34.8 ± 2.6	35.0	14.01 ± 0.16	1.58
Tri			(5734)	(214)	(2758)				(101)	
88POS79	Ap	25	2.548	2.801	4.026	47.7	31.2 ± 3.0	20.7	13.98 ± 0.21	1.55
Kk			(5734)	(123)	(1768)				(54)	
91POS61	Ap	20	1.670	2.405	1.777	98.5	39.7 ± 8.9	13.9	14.38 ± 0.26	0.51
Tri			(2630)	(23)	(170)				(4)	
Outcrop—Front range of Sadlerochit Mountains										
91POS70	Ap	20	1.672	3.577	2.384	57.7	44.1 ± 2.9	18.7	14.35 ± 0.12	1.19
Kh			(2630)	(303)	(2019)				(107)	
91POS71	Ap	20	1.673	4.700	3.805	97.1	36.3 ± 3.1	29.8	14.11 ± 0.13	1.16
Kk			(2630)	(168)	(1360)				(101)	
91POS72	Ap	20	1.457	5.084	5.009	99.9	26.0 ± 1.9	45.0	14.16 ± 0.08	0.80
Kk			(2329)	(231)	(2276)				(100)	
91POS73	Ap	25	2.507	0.900	1.450	95.1	28.1 ± 3.2	17.2	14.23 ± 0.15	1.16
Kk			(8109)	(81)	(1312)				(101)	
91POS74	Ap	20	1.465	2.245	2.254	99.9	25.7 ± 5.3	20.2	14.03 ± 0.28	0.56
Tri			(2329)	(26)	(261)				(4)	
91POS74	Zi	10	0.683	150.4	9.005	0.2	51.0 ± 2.8	686.3	N.D.	N.D.
Tri			(2662)	(2652)	(1588)					
91POS75	Ap	20	1.675	4.729	2.746	98.5	50.7 ± 4.1	21.5	13.90 ± 0.11	1.07
TKc			(2630)	(197)	(1144)				(81)	
91POS76	Ap	25	1.472	3.160	1.700	58.2	48.1 ± 4.1	15.1	13.88 ± 0.13	1.15
TKc			(2329)	(179)	(963)				(82)	
91POS77	Ap	25	1.602	1.596	1.709	99.9	26.3 ± 2.8	14.0	14.44 ± 0.11	1.10
Tri			(3605)	(102)	(1092)				(105)	
91POS77	Zi	10	0.735	0.399	2.730	24.1	47.4 ± 3.1	292.3	N.D.	N.D.
Tri			(2717)	(760)	(521)					
91POS78	Ap	25	1.602	1.403	1.459	99.9	27.1 ± 3.1	11.9	14.31 ± 0.18	0.86
Pe			(3605)	(89)	(926)				(23)	
91POS79	Ap	25	1.602	2.256	2.069	93.8	30.7 ± 3.0	16.9	14.83 ± 0.12	1.25
JKk			(3605)	(119)	(1092)				(102)	
91POS80	Ap	25	1.602	2.420	2.376	70.0	28.7 ± 2.4	19.4	14.36 ± 0.12	1.22
TKc			(3605)	(164)	(1610)				(101)	
91POS81	Ap	25	1.602	2.364	1.500	99.3	44.4 ± 4.3	12.3	14.38 ± 0.29	1.66
TKc			(3605)	(127)	(806)				(32)	
Beli Unit #1 Well										
93-1	Ap	25	2.588	0.510	2.880	64.5	85.3 ± 6.7	15.7	13.87 ± 0.12	1.22
Ts			(10,891)	(171)	(966)				(105)	
93-2	Ap	25	2.588	0.970	2.834	99.4	71.4 ± 8.8	12.2	13.02 ± 0.16	1.45
Ts			(10,891)	(123)	(917)				(85)	
93-3	Ap	25	2.588	0.560	1.455	98.6	51.8 ± 6.5	15.4	11.80 ± 0.19	2.45
TKc			(10,891)	(111)	(876)				(76)	
93-4	Ap	25	2.588	0.670	1.457	52.3	20.8 ± 7.1	18.9	10.57 ± 0.45	2.33
Kh			(10,891)	(42)	(1032)				(54)	
93-5	Ap	19	2.588	0.070	1.712	59.1	8.3 ± 4.2	12.2	N.D.	N.D.
Tri			(10,891)	(9)	(266)				(0)	

Note: Standard and induced track densities measured on mica external detectors, and fossil track densities measured on internal mineral surfaces. Brackets show number of tracks counted. Ages for apatite samples (Ap) calculated by using $\zeta = 352.7 \pm 4$ for dosimeter glass SRM612 or $\zeta = 379.2 \pm 3$ for dosimeter glass CN5 (analyst: P. O'Sullivan). Ages for zircon samples (Zi) calculated using $\zeta = 87.8 \pm 7.5$ for dosimeter glass U3 (analyst: P. O'Sullivan). Errors quoted at $\pm 1\sigma$. N.D.—not determined.

†Unit: Ts—Tertiary Sagavanirktok Formation;TKc—Tertiary–Cretaceous Canning Formation; Kh—Cretaceous Hue Shale; Kk—Cretaceous Kemik Sandstone; JKk—Jurassic Kingak Shale; Tri—Triassic Ivishak Formation; and Pe—Permian Echooka Formation.

also take into account the complex thrust faulting in the area. Rocks collected from the Canning Formation between and north of the transects and in the northern part of the Katakturuk River transect gave ages of ca. 44–51 Ma, as did the northernmost sample along the Marsh Creek transect, a sample from the Hue Shale (Fig. 5). However, rocks from deeper stratigraphic levels only a few kilometers to the south along both transects gave ages of ca. 31–26 Ma. The distributions of confined-track lengths were very narrow; standard deviations were <1.3 μm for all except one sample (sample 81 from the Cretaceous Canning Formation) (Fig. 8). Furthermore, little difference in the characteristic shape of the distributions of confined-track lengths is evident for samples with significantly different AFTT ages or for samples from different structural positions and elevations, which indicates that all of the sampled rocks cooled quickly irrespective of their present location.

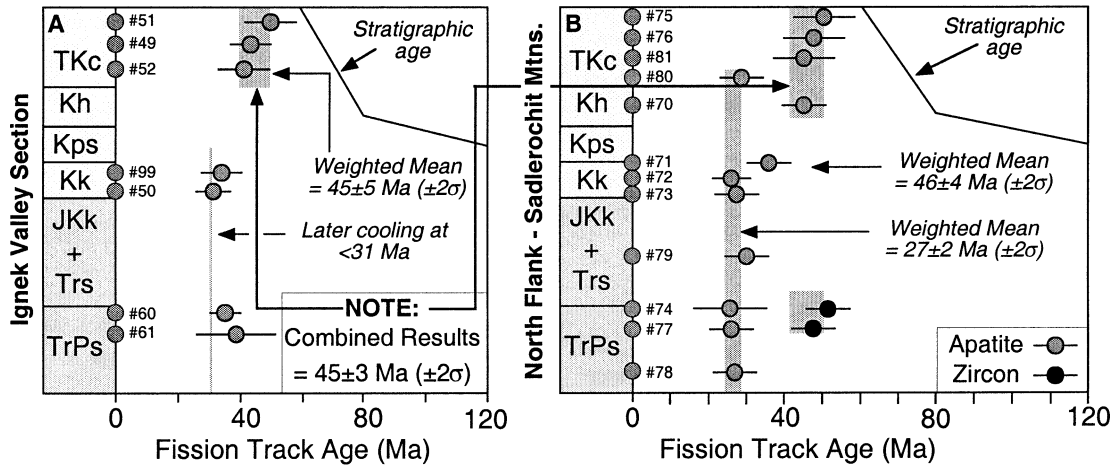

Figure 7. Fission-track ages for samples from (A) the Ignek Valley and (B) the north flank of the Sadlerochit Mountains, plotted against their relative position in the stratigraphic section and against stratigraphic age. Symbols: TKc—Tertiary–Cretaceous Canning Formation, Kh—Cretaceous Hue Shale, Kps—Cretaceous pebble shale unit, Kk—Cretaceous Kemik Sandstone, JKk—Jurassic Kingak Shale, Trs—Triassic Shublik Formation, and TrPs—Permian–Triassic Sadlerochit Group. Stratigraphic thicknesses are extrapolated from those present in the Beli Unit #1 well. Error bars are ±2σ. Shaded areas represent the age limits of each cooling event.

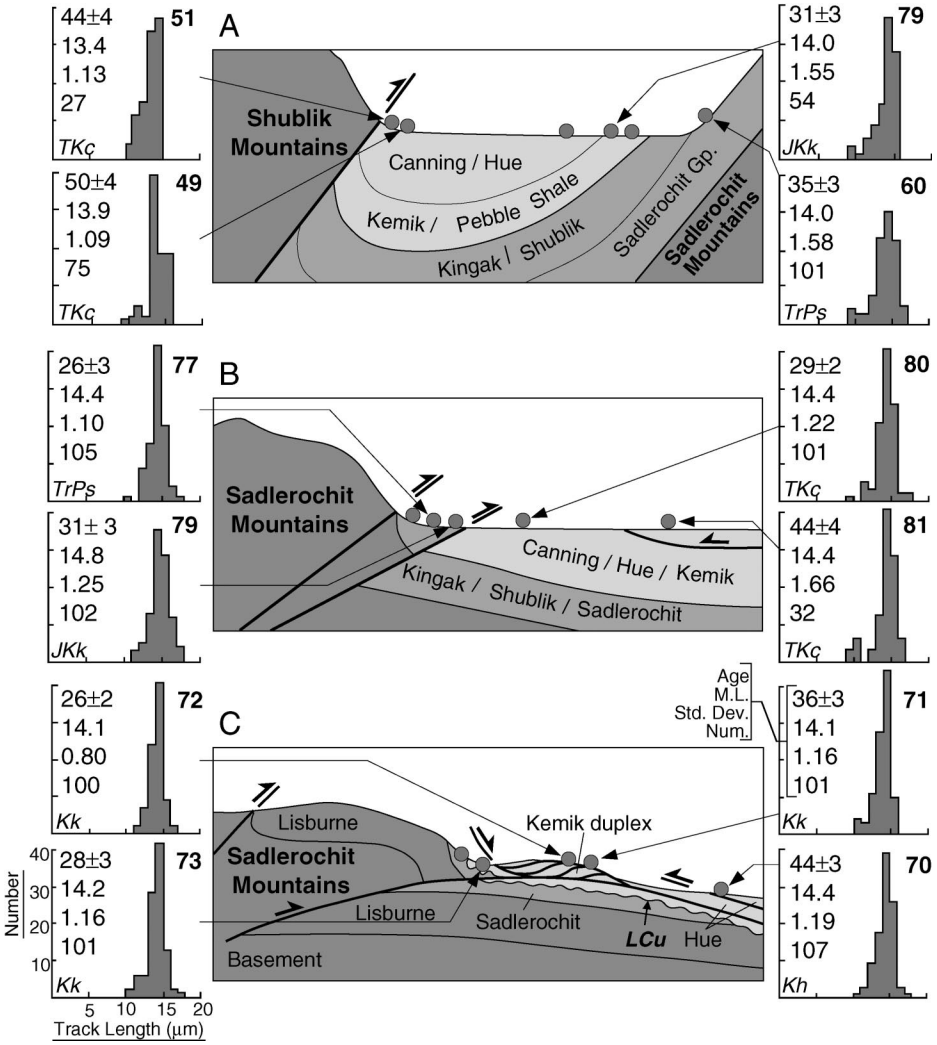

Figure 8. Representative AFTT results from the Sadlerochit Mountains region plotted along schematic cross sections: (A) Ignek Valley, (B) Katakturuk River transect, (C) Marsh Creek transect (not to scale). For each sample, the distribution of confined-track lengths, AFTT age, mean track length, standard deviation, and number of confined tracks measured are shown. Track lengths are in micrometers, and distributions are normalized to 100 tracks. Errors are ±1σ. Symbols for the different stratigraphic units are presented with Figure 7.

Interpretation of the AFTT data from the north flank of the Sadlerochit Mountains suggests that each of the apatite ages was totally reset following deposition owing to exposure to elevated paleotemperatures of >110 °C. Application of the track-annealing model of Laslett et al. (1987) suggests that, to preserve the long mean lengths and the narrow distributions, each of the samples must have (1) cooled rapidly (in <5 m.y.) from the proposed maximum paleotemperatures to temperatures of ≤50 °C at the time suggested by the AFTT ages, and (2) subsequently remained at temperatures of less than ~50 °C. In the case of samples collected from the upper part of the Canning Formation, as well as the Hue Shale sample on the Marsh Creek transect, rapid cooling must have occurred at ca. 45 Ma, whereas samples collected from lower stratigraphic levels along each transect did not finally cool below ~110 °C until ca. 27 Ma.

Zircon Fission-Track Samples from the North Flank of the Sadlerochit Mountains

Six zircon fission-track thermochronology (ZFTT) analyses were also completed to determine the high-temperature thermotectonic history of the rocks exposed within the Sadlerochit Mountains. Of the six, four analyses resulted in ZFTT ages greater than or equal to the depositional age of the rock, which indicates that the rocks did not reach sufficient temperatures (>180–225 °C) after burial to significantly reduce the apparent ages of the detrital zircons within the samples. These results will not be discussed further because they provide no insights into the timing of unroofing. However, two samples from the Triassic Ivishak Formation (samples 74 and 77) gave ZFTT ages significantly younger than depositional ages (51 ± 3 Ma and 47 ± 3 Ma, respectively). Both samples contained similar zircon-grain age populations, including a distinct population of grains that were younger (ca. 45 Ma) as well as a few older grains with ages up to ca. 70 Ma (Fig. 9). We interpret the older grains in each sample as being only partially reset, whereas the younger grains were totally reset and record the time of cooling. Therefore, these particular rocks previously resided at maximum paleotemperatures prior to ca. 45 Ma, after which they cooled below ~225 °C at approximately the same time that rocks at higher stratigraphic levels (Canning Formation and Hue Shale to east) cooled below ~110 °C. The AFTT ages of 26 ± 5 and 26 ± 3 Ma for sample 74 and 77, respectively, indicate that these rocks did not cool below ~110 °C until much later.

Apatite Fission-Track Samples from the Beli Unit #1 Well

Apatite fission-track ages from the Beli Unit #1 well range between 85 ± 7 Ma, at an estimated present temperature of ~16 °C at 1005 m depth, and 8 ± 4 Ma, at an estimated present temperature of ~94 °C at 3630 m depth (Fig. 10). Estimated present temperatures were determined by using a geothermal gradient of ~27 °C/km calculated from a corrected bottom-hole temperature (BHT) of ~104 °C at 4502 m depth and a mean annual surface temperature of ~–9 °C reported by Magoon et al. (1987).

The AFTT parameters plotted against sample depth and present temperature in Figure 10 indicate that samples from the Beli Unit #1 well must previously have been exposed to elevated paleotemperatures following deposition. For instance, the AFTT ages from the deepest three samples were all significantly less than the stratigraphic ages. Additionally, the mean confined-track lengths were shorter than would be expected if they had formed at the prevailing temperatures. In principle, lower-than-expected mean confined-track lengths could reflect inheritance of shorter tracks from source-terrane rocks, or, alternatively, the samples may have been subjected to postdeposition paleotemperatures sufficiently high to produce the observed reduction in mean confined-track length. The AFTT ages from the three deepest samples are less than their respective stratigraphic ages, so the discrepancy cannot be explained in terms of short tracks inherited from source terranes and must therefore be due to the effects of enhanced fission-track annealing at elevated paleotemperatures after deposition. This interpretation is supported by R_o values from the well that range between ~0.47% at 70 m depth and ~1.60% at 4.3 km depth (Magoon et al., 1987). These values indicate that rocks in the well were previously exposed to maximum paleotemperatures of ~75–85 °C at 70 m depth and >170 °C at 4.3 km depth. These temperatures are significantly higher than estimated present temperatures of −7 °C and 99 °C, respectively.

Application of the track-annealing model of Laslett et al. (1987) to the AFTT data from the shallowest two samples suggests that during the early to middle Eocene, these samples were exposed to maximum paleotemperatures of ~80–95 °C prior to rapid cooling. The best match for the available data suggests that cooling on the order of ~35–45 °C occurred over ~5–10 m.y. at some time between ca. 50 and 40 Ma. Data from the three deepest samples collected from the well suggest that they were subjected to paleotemperatures of ≥110 °C after deposition and were subsequently cooled to present temperatures. For example, modeling of the fission-track data from sample 93–3 suggests that the sample initially cooled by ~35–45 °C over ~5–10 m.y. from maximum paleotemperatures of ~110 °C at some time between ca. 50 and 40 Ma.

DISCUSSION OF FISSION-TRACK INTERPRETATIONS

Interpretation of the fission-track data suggests that (1) all of the rocks collected from Ignek Valley and along the northern flank of the Sadlerochit Mountains were previously exposed to elevated paleotemperatures of ≥110 °C, and (2) at least two of the rocks collected at the northern foot of the Sadlerochit Mountains were previously exposed to temperatures as high as ~225 °C. Furthermore, these rocks must have subsequently undergone at least two major episodes of rapid cooling to bring them to present surface conditions.

Evidence for Elevated Paleotemperatures

Vitrinite reflectance data from Magoon et al. (1987) and from this study provide additional evidence that the rocks sampled throughout the Sadlerochit Mountains were previously exposed to significantly elevated paleotemperatures (Fig. 5). For instance, R_o values from Ignek Valley range from 1.6% in the Shublik Formation to 0.8% in the Canning Formation. These values indicate that the samples had been exposed to maximum paleotemperatures of ~120–185 °C, which are more than sufficient to account for the proposed resetting of the AFTT ages from Ignek Valley. Along the northern flank of the Sadlerochit Mountains, R_o values from the top of the preserved section in the Canning Formation range between ~0.6% and 0.71%, which suggests exposure to maximum paleotemperatures of ~95–115 °C. These temperatures are again sufficient to account for the proposed resetting of the AFTT ages, particularly because the apatites dated were primarily F rich (Fig. 6). Down section, the R_o values increase to as high as 2.5% and 2.6% at the base of the sampled section in the Sadlerochit Group (Fig. 5). Such values suggest that these particular rocks were exposed

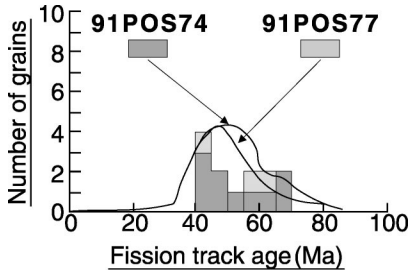

Figure 9. ZFTT results from samples 74 and 77 collected along the northern flank of the Sadlerochit Mountains.

to paleotemperatures as high as ~225 °C, which are sufficient to account for the resetting of both the AFTT and ZFTT ages.

Cooling History of Surface Samples

We propose that rocks from the study area have Cenozoic thermal histories similar to those shown in Figure 11. Following exposure to elevated paleotemperatures of ≥110 °C, rocks now exposed throughout the Sadlerochit Mountains region must have undergone significant cooling via denudation to bring them to present surface conditions. The timing of two proposed major cooling episodes is shown by the plot of fission-track age relative to stratigraphic position (Fig. 7). Samples collected from the Canning Formation in Ignek Valley and north of the Sadlerochit Mountains front, as well as a sample from Hue Shale on the eastern Marsh Creek transect, record rapid cooling from elevated paleotemperatures of >110 °C to <50 °C at ca. 45 Ma. The AFTT ages from all of these samples are concordant; the weighted mean age of ca. 45 ± 3 Ma suggests that they all record the same cooling episode independent of location. However, samples collected from deeper stratigraphic levels throughout the region record a later episode of rapid cooling from elevated paleotemperatures of >110 °C at ca. 27 Ma. The timing of this second event is defined by concordant cooling ages with a weighted mean age of ca. 27 ± 2 Ma from samples from the north flank of the Sadlerochit Mountains.

Cooling and Burial History of the Beli Unit #1 Well

As explained earlier, the slope of the fitted linear relationship between maximum paleotemperature and present depth provides a direct estimate of the maximum paleogeothermal gradient prior to cooling. As shown in Figure 12, the estimated maximum paleogeothermal gradient of ~28 °C/km is similar to the estimated present-day geothermal gradient of ~25 °C/km. This finding suggests that basin heat flow has not changed significantly since maximum paleotemperatures were reached; however, a great deal of section must have been removed because the maximum geothermal gradient is offset toward higher temperatures owing to previous exposure to elevated temperatures. Because any change in the geothermal gradient since the time of maximum paleotemperatures has been negligible, the amount of section removed can be estimated by dividing the amount of cooling by the estimated maximum geothermal gradient (O'Sullivan, 1999). If a geothermal gradient of ~28 °C/km is used, the section in the Beli Unit #1 well is calculated to have cooled to present temperature conditions because of ~1.5 km of denudation (Fig. 12).

Figure 13 shows the proposed burial history for the Beli Unit #1 well, as defined by the regional stratigraphy, AFTT, and vitrinite-reflectance data. The section in Beli Unit #1 well was subjected to maximum paleotemperatures during the early Eocene, at which time sedimentary rocks of the Sagavanirktok Formation and the upper part of the Canning Formation remained at paleotemperatures of ≤110 °C, whereas the lower part of the Canning Formation and deeper rock units were exposed to paleotemperatures of >110 °C. In the Eocene at some time between ca. 50 and 40 Ma, the entire section was cooled by ~30–

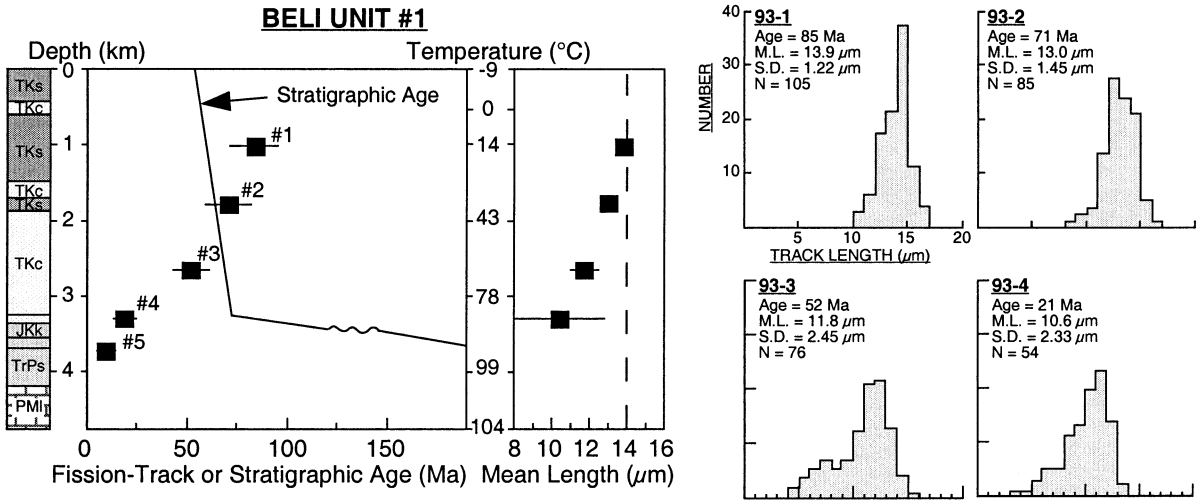

Figure 10. Composite figure showing fission-track parameters (solid squares—age and track length) plotted against sample depth and present-day temperature for samples from the Beli Unit #1 well. Variation of stratigraphic age with depth is shown as solid line in central panel. Error bars are ±2σ. Symbols: TKs—Sagavanirktok Formation, TKc—Canning Formation, JKk—Kingak Shale, TrPs—Sadlerochit Group, PMi—Lisburne Group. Information shown with each track-length distribution includes fission-track age (Ma), mean confined-track length (μm), standard deviation (μm), and number of confined tracks measured. Track-length distributions are normalized to 100 tracks (labeled as Number on the *y*-axis of the track-length distributions; actual number given by *n* values).

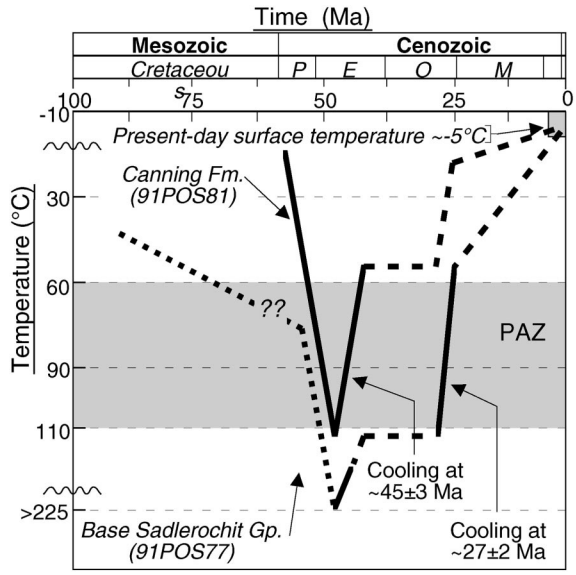

Figure 11. Proposed time vs. temperature history of rocks from the Sadlerochit Mountains region. Results from two representative samples are shown, 91POS77 from the base of the sampled section in the Triassic Ivishak Formation and 91POS81 from the top of the section in the Cretaceous Canning Formation. The burial path for the Canning Formation is assumed on the basis of the burial history path deduced from the Beli Unit #1 well. It is likely that the Ivishak Formation had a similar burial history since the Cretaceous because deposition of the Brookian sediments was responsible for burying the underlying units to maximum paleotemperatures (Magoon et al., 1987). Solid lines represent where the thermal history is tightly controlled, whereas dashed lines represent little control. PAZ represents the AFTT partial annealing zone (~60–110 °C) in which fission tracks in apatite undergo accelerated annealing. At temperatures below ~60 °C, fission tracks in apatite anneal but at a rate where little reduction in the AFTT age is observed. At temperatures of ~110 °C, at the base of the PAZ, tracks anneal rapidly, resulting in a zero apparent age. See text for additional details.

40 °C in ~5 m.y. owing to ~1.3–1.5 km of denudation. The concordant ages and close proximity support the interpretation that the episode of cooling recorded by the well data is the same as the event at ca. 45 ± 3 Ma recorded by the outcrop samples north and south of the Sadlerochit Mountains. Finally, during the late Miocene, the stratigraphic section underwent ~10–15 °C of cooling in response to regional climatic change (e.g., O'Sullivan and Brown, 1998). Minor cooling has subsequently brought the rocks to present temperature conditions.

STRUCTURAL INTERPRETATION

Fission-track data can provide some important limits on the timing and magnitude of structural displacements and clarification of relative timing where it is not evident from crosscutting geologic relationships. These limits on structural interpretations depend on the important assumption that the cooling events recorded by the fission-track data, particularly those that are interpreted to be rapid, reflect rapid erosional unroofing driven by the creation of tectonic relief. Creation of tectonic relief results in rock uplift, but related changes in topographic relief depend on the balance between the rates of rock uplift and unroofing (England and Molnar, 1990). Thus, the fission-track data may provide insights into the age, rate, amount, and location of unroofing, but do not provide a direct indication of paleotopography.

For the purposes of determining amounts of unroofing or burial, we used the following values (as already discussed): (1) The paleogeothermal gradient was 28 °C/km. (2) A partial annealing zone (PAZ) for apatite of ~60–110 °C would be at a depth of ~2–4 km. Apatites below the PAZ would be fully annealed, whereas no annealing would occur above the PAZ. (3) A PAZ for zircon is not so well established, but we assume the possibility of partial annealing over a temperature range of 180–225 °C, for a depth range of ~6–8 km.

These depths provide a basis to assume the following restrictions on structural interpretations: (1) Evidence of rapid cooling (<5 m.y.) by AFTT implies structural uplift sufficient to drive ≥2 km of unroofing to bring the sample within ≤2 km of the surface. (2) Partially reset AFTT ages imply uplift to within ~2–4 km of the surface at some time prior to the oldest age, followed by unroofing to within ≤2 km of the surface at some time after the youngest age. (3) Discordant AFTT and ZFTT ages in the same sample imply unroofing to within 4–8 km of the surface at a time at least as old as the ZFTT age, followed by unroofing to within ≤2 km of the surface at a time indicated by the AFTT age, if it is assumed that the AFTT data indicate rapid cooling.

Even if the essential assumption that the fission-track ages reflect tectonically driven unroofing is accepted, these limits are only approximations, subject to the uncertainty and variability in both the thermal history of each sample and the paleogeothermal gradient. However, these limits are more likely to be valid if multiple samples define a reasonably consistent pattern of ages and thermal histories relative to the structures in an area. Such patterns can be identified in the different areas addressed by this study. These patterns are most usefully defined and analyzed if the locations of samples are projected along structural strike into their appropriate structural position on a structural section oriented perpendicular to strike (Fig. 8). This approach provides the most appropriate frame of reference to assess the different thermal histories of the samples on the basis of their positions relative to important structures and their displacements. Samples were grouped according to each of the three areas sampled in this study (the Katakturuk River transect, the Marsh Creek transect, and Ignek Valley) because structures are relatively consistent along strike in each area.

Northern Sadlerochit Mountains

The fission-track data from the two areas along the northern front of the Sadlerochit Mountains—the Katakturuk and Marsh Creek transects—display very similar patterns of distribution relative to the topographic range front and stratigraphy (Figs. 3, 5). Along both transects, samples >2.5 km north of the local range front yield AFTT ages of ca. 45 Ma, whereas samples <2.5 km north of the local range front yield AFTT ages of ca. 27 Ma. The local structure and stratigraphy must be considered in interpreting the fission-track data along each transect. A critical distinction is that the topographic range front in each area is controlled by different structures. The topographic range front is controlled by the Sadlerochit Mountains thrust along the Katakturuk River transect, but is 5 km north of and not related to that thrust along the Marsh Creek transect. To the west, along the Katak-

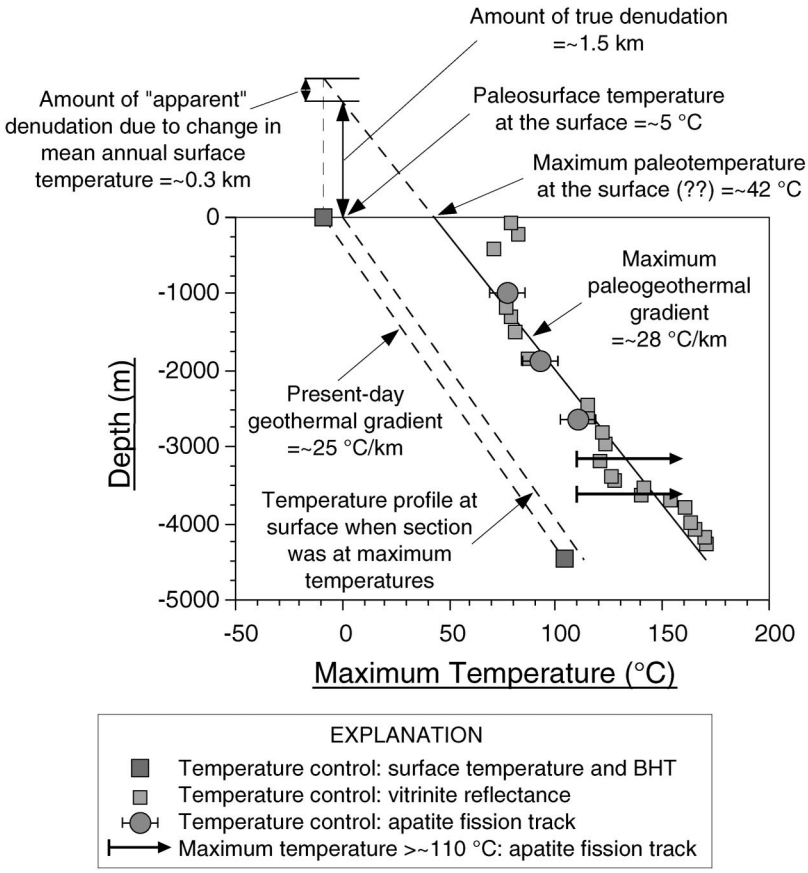

Figure 12. Estimated maximum paleotemperature profile in the Beli Unit #1 well, derived from available fission-track and vitrinite-reflectance values, plotted against sample depth. For comparison, the present-day geothermal gradient in the well, and the projected paleogeothermal gradient in the well at the time the stratigraphic section was exposed to maximum paleotemperatures are also shown. Original vitrinite-reflectance values from Magoon et al. (1987). Estimated maximum paleotemperatures from R_o data were determined using the model proposed by Burnham and Sweeney (1989; their equation 2). Symbols: FT—fission-track, BHT—bottom-hole temperature. See text for details.

turuk River transect, the samples from the ca. 45 Ma age group are from the upper, sandy part of the Canning Formation and lie above and north of a north-dipping structural detachment within the Canning Formation (''Katakturuk thrust fault'' of Kelley and Foland, 1987). Samples from the ca. 27 Ma age group lie between this detachment and the Sadlerochit Mountains thrust fault and are from the lower, finer-grained part of the Canning Formation, the Kingak Shale, and the Sadlerochit Group.

To the east, along the Marsh Creek transect, the sample from the ca. 45 Ma age group is from the Hue Shale and lies above and north of a north-dipping structural detachment within the Hue Shale (''Nularvik thrust fault'' of Kelley and Foland, 1987). Samples from the ca. 27 Ma age group lie below this detachment and are from the Kemik Sandstone and the Sadlerochit Group. The two northern samples from the Kemik Sandstone are from a duplex bounded between detachments in the Kingak Shale and pebble-shale unit that is interpreted to have been displaced from the south side of the Sadlerochit Mountains (Kelley and Foland, 1987; Mull, 1987; Meigs, 1989). It is important to note that the two southernmost samples in the ca. 27 Ma age group lie in the footwall immediately beneath this duplex. They are from the Kemik Sandstone and Sadlerochit Group and are at the top of a structurally intact stratigraphic section that continues downward into basement. Along each transect, a sample from the Sadlerochit Group at the range front yields a ZFTT age of ca. 45 Ma and an AFTT age of ca. 27 Ma.

The AFTT data suggest that two distinct unroofing events are recorded in different parts of the stratigraphic section: (1) $\geq$2 km unroofing to $\leq$2 km depth at ca. 45 Ma in strata upward from the upper part of the Canning to the west and the Hue Shale to the east, and (2) $\geq$2 km unroofing to $\leq$2 km depth at ca. 27 Ma in strata downward from the lower part of the Canning to the west and the Kemik to the east.

The AFTT and ZFTT ages from the Sadlerochit Group at the range front suggest that these rocks were unroofed to within ~4–8 km of the surface at ca. 45 Ma and then to $\leq$2 km of the surface at ca. 27 Ma. These rocks must have remained at $\geq$2 km below the stratigraphically higher rocks that yielded apatite ages of ca. 45 Ma.

These interpretations have several structurally important implications. The ca. 45 Ma ages are from stratigraphically higher rocks compared to the ca. 27 Ma ages. Younger-over-older structural detachments or older-over-younger thrust faults separate some of the samples. The detachments do not disrupt the stratigraphic order, although some structural thickening has occurred between detachments. The thrust faults

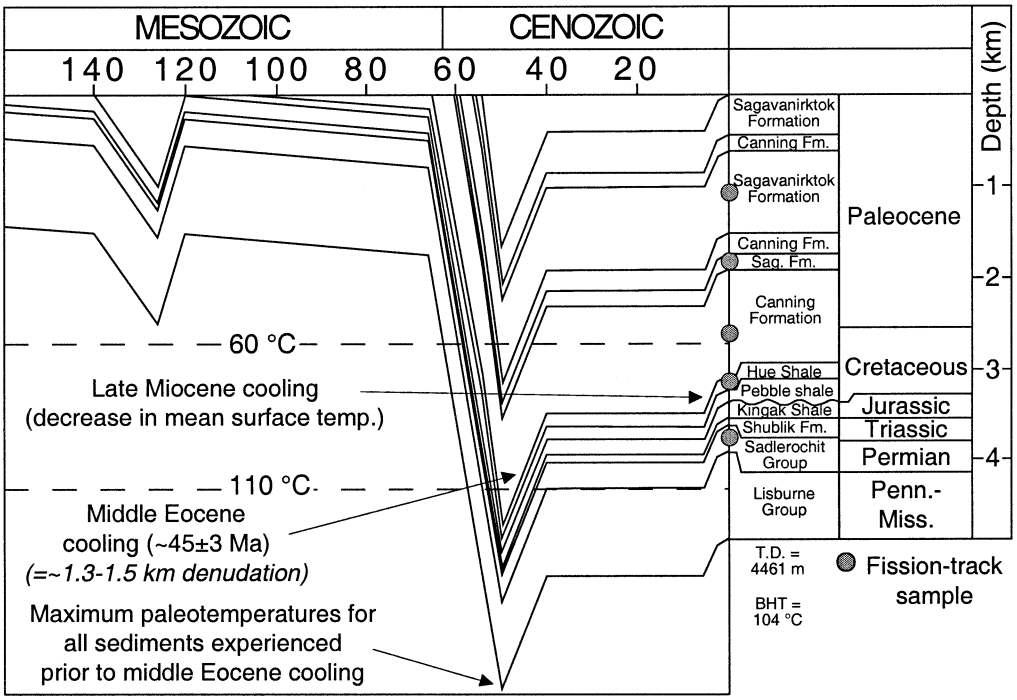

Figure 13. Proposed depositional history for Beli Unit #1 well based on fission-track, vitrinite-reflectance, and stratigraphic parameters. Results suggest that maximum paleotemperatures were reached in the early Eocene prior to rapid cooling in response to kilometer-scale denudation starting in the middle Eocene. Symbols: BHT—bottom-hole temperature, T.D.—total depth to bottom of well. See text for details.

do not cut across large thicknesses of stratigraphic section, nor do they coincide with the boundaries between the two age groups. In the absence of duplication or omission of significant thicknesses of stratigraphic section, the earlier cooling of stratigraphically higher rocks could have resulted either from simple unroofing of a structural section or from juxtaposition of rocks that cooled at different times across a structural detachment localized along a stratigraphic horizon. The first possibility can be eliminated because the present cross-strike distances between samples in the two age groups are too small to allow them to be separated by a structural thickness of 2 km (Fig. 5). If the different ages represented two distinct periods of rapid unroofing of a structural section, then samples that indicate rapid cooling during each event should be separated by at least 2 km of structural section, representing the apatite PAZ. The cross-strike distance between samples represents the maximum possible structural separation that could exist between the samples, if it is assumed that the section was tilted to vertical during or following the second cooling event. However, the mapped distribution of rock units and the observed dips indicate much less tilt, probably no more than 15°N dip, except in the steeply dipping beds at the range front (Fig. 8). Thus, the separation between the structural levels of the samples is actually much less than the cross-strike distance, assuming that no more than the observed tilt occurred during or since the later cooling event.

A further implication is that insufficient structural section separates the two age groups to account for the older cooling event simply by structural thickening above a detachment that separates the two age groups. Small-scale folds and thrust faults indicate significant structural thickening up section from the Kingak Shale. However, this duplication of section appears to be confined between structural detachments in the Kingak Shale, pebble shale, Hue Shale, and Canning Formation (Fig. 3) (Kelley and Foland, 1987; Meigs, 1989; Wallace and Hanks, 1990). This thickening is confined to intervals of relatively small stratigraphic thickness, and the observed distance that now separates detachments indicates that kilometer-scale structural thickening has not occurred between them.

The close juxtaposition of samples from the two age groups implies that they were juxtaposed across an intervening fault at ca. 27 Ma or later. Several possibilities exist to account for such a fault.

1. A normal fault from the north limb of the Sadlerochit Mountains anticlinorium could root into a detachment down section to the north. This possibility might allow stratigraphically higher rocks that cooled during early growth of the Sadlerochit Mountains anticlinorium to be emplaced over stratigraphically lower rocks that cooled during later growth of the anticlinorium. No evidence has been observed for such normal faulting, although it could have been removed by erosion of the forelimb of the anticlinorium. Another problem with this idea is that rocks would be expected to cool progressively from north to south with increasing displacement of the horse that underlies the anticlinorium. However, the cooling ages observed across the hypothesized south-over-north normal fault would indicate earlier cooling to the south.

2. Stratigraphically older beds could have been thrust northward over younger beds on a large-displacement thrust fault near the range front. South-dipping thrusts are either observed or possible near the range front along both transects, but these are not located where they could account for the observed juxtaposition of the different age groups. Along the Marsh Creek transect, the Kemik duplex has a large horizontal displacement and could potentially be only the base of a much thicker displaced section. However, the thickness between the ca. 27 Ma samples in the Kemik duplex and the ca. 45 Ma sample in the overlying Hue Shale is too small to account for ca. 45 Ma cooling by thickening in the Kemik duplex. Samples in and immediately below the Kemik duplex have ca. 27 Ma ages. This fact suggests that emplacement of the Kemik duplex alone cannot account for cooling at ca. 27 Ma. Along the Katakturuk River transect, the Sadlerochit Mountains fault and its splays lie south of the boundary between the ca. 27

Ma and ca. 45 Ma age groups and so cannot account for their juxtaposition.

3. Stratigraphically older beds could have been thrust northward in a basement-cored wedge that was inserted beneath younger beds that overlie a detachment with backthrust displacement. Younger ages in the wedge could record cooling during its emplacement beneath earlier-cooled cover rocks. Such triangle-zone or passive-roof duplex geometries (Jones, 1982, 1996; Banks and Warburton, 1986; Cooper, 1996) are common in the frontal parts of fold-and-thrust belts worldwide. An analogous geometry has been proposed for the subsurface to the north on the basis of seismic data (Fig. 4B) (Bruns et al., 1987; Kelley and Foland, 1987; Potter et al., 1999). Kelley and Foland (1987) identified several appropriately oriented detachments north of the Sadlerochit Mountains, although they interpreted only the intra-Canning detachment to have a backthrust displacement.

We prefer the triangle-zone interpretation because it most easily accounts for the observations. However, both this interpretation and the south-dipping thrust interpretation require cooling of younger beds to the north while even slightly older beds to the south remained at sufficient depth to show no evidence of cooling from the AFTT data. This circumstance implies that greater structural relief was created to the north than to the south at ca. 45 Ma, whereas greater structural relief was created to the south than to the north at ca. 27 Ma. This pattern suggests a departure from the forward-propagating thrust sequence that is commonly assumed for fold-and-thrust belts, including the northeastern Brooks Range.

An additional important implication is that basement likely was involved in creating the necessary structural relief during each event. Cooling of apatite at ca. 27 Ma is recorded by samples from the Sadlerochit Group, which in the Sadlerochit Mountains is not separated by a significant structural detachment from the basement (Meigs, 1989; Wallace and Hanks, 1990; Wallace, 1993). Thus, strata in the Sadlerochit serve as a stratigraphically higher marker for basement-involved structures. The same samples from the Sadlerochit also record ca. 45 Ma cooling of zircon, reflecting deeper-seated basement involvement in the same rocks during this earlier event. The evidence that ca. 45 Ma cooling of apatite also resulted from basement-involved structures is more tenuous because these ages are recorded in stratigraphically higher rocks that are separated by multiple detachment horizons from the underlying basement. However, as already explained, the amount of structural thickening between these detachments probably is not enough by itself to account for the cooling.

Another important observation is the great similarity in the relationship between thermal history and stratigraphic and structural position along the Katakturuk River and Marsh Creek transects. This observation suggests that similar structures influenced the thermal history along each transect. However, a key structural difference exists between the transects. The southernmost sample in the Marsh Creek transect lies almost 5 km north of the Sadlerochit Mountains thrust, so that fault is unlikely to have had any influence on the thermal history of the transect (Figs. 5, 8). The southernmost sample in the Katakturuk River transect lies immediately north of the same thrust and is in its footwall. It is possible that at least some of the ca. 27 Ma cooling recorded in overturned beds in the footwall of the thrust resulted from formation of a footwall syncline, although it is unlikely that this structure alone resulted in $\geq$2 km of structural relief. It is important to note that no fission-track samples have been dated in the hanging wall near the thrust because of the lack of appropriate lithologies, so the available fission-track data provide no firm evidence for the time of movement on the thrust fault.

Another difference between the transects is that the break between ca. 45 and ca. 27 Ma ages is within the Canning Formation along the Katakturuk River transect, but beneath the Hue Shale along the Marsh Creek transect. Although the structures along both transects are broadly equivalent, sufficient distance and structural difference exist between the two transects to account for the different stratigraphic position in the age break by differences along strike in local structural relief and/or detachment positions.

Ignek Valley

The samples from Ignek Valley all lie within 5 km to the north of the Shublik Mountains thrust (Figs. 5, 8). This position is analogous to that of the northern Sadlerochit Mountains samples relative to the Sadlerochit Mountains thrust. However, some key differences exist between the structures and the associated fission-track results. The main structural difference is that the northernmost samples lie within the lower part of the gently south-dipping backlimb of the Sadlerochit Mountains anticlinorium.

Samples from the Canning Formation and $<$2 km north of the Shublik Mountains range front yield AFTT ages of ca. 45 Ma. Samples from the Kemik Sandstone and Sadlerochit Group and $>$2 km from the range front yield mixed AFTT ages with a range of 40–31 Ma. Final cooling of these samples probably occurred after ca. 31 Ma, the youngest of these ages.

The apatite fission-track data record different thermal histories in different parts of the stratigraphic section: (1) $\geq$2 km unroofing to $\leq$2 km depth at ca. 45 Ma in the Canning Formation, and (2) $\geq$2 km unroofing to $\sim$2–4 km depth at ca. 45 Ma followed by unroofing to $\leq$2 km depth at some time after ca. 31 Ma in the Kemik Sandstone and Sadlerochit Group.

As in the northern Sadlerochit Mountains, the samples that cooled rapidly at ca. 45 Ma are in the upper part of both the stratigraphic section and the present structural section. In contrast with the northern Sadlerochit Mountains, the samples lower in the section were unroofed sufficiently at ca. 45 Ma to result in partial resetting and thus provide only a maximum age for later unroofing. The stratigraphically and structurally higher rocks that cooled rapidly at ca. 45 Ma lie closer to the Shublik Mountains fault and to the south of the lower rocks that were partially reset. In the northern Sadlerochit Mountains, by contrast, the stratigraphically and structurally higher rocks that cooled rapidly at ca. 45 Ma lie farther from the Sadlerochit Mountains fault and to the north of the lower rocks that cooled rapidly at ca. 27 Ma.

The cross-sectional distribution of the two groups of samples in Ignek Valley (Fig. 8), and the small amount of structural section that separates them, allows the differences in the thermal histories of the two groups to be interpreted to be the result of simple unroofing of a structural section. Although clear evidence exists in Ignek Valley for structural thickening above detachments in the Kingak and Hue Shales (Mull, 1987; Robinson et al., 1989; Rogers, 1992), this thickening is not sufficient by itself to account for the rapid cooling of the Canning Formation at ca. 45 Ma and the probably synchronous passage of section from the Sadlerochit through the Kemik into the apatite PAZ (Figs. 3, 8). This interpretation implies at least some uplift in Ignek Valley above a detachment somewhere beneath the Sadlerochit Group. However, exposures within the backlimb of the Sadlerochit Mountains anticlinorium indicate that no significant detachment has occurred there

between the Sadlerochit Group and the basement. Thus, displacement above a detachment in the basement must be called upon to account for any tilting or displacement of the backlimb that may have influenced the fission-track ages from Ignek Valley.

The structural and fission-track data suggest two possible structural scenarios to account for uplift in Ignek Valley at ca. 45 Ma. The first involves northward emplacement of the leading edge of the Shublik Mountains horse as a wedge beneath a detachment in the Kayak Shale (Wallace and Hanks, 1990; Rogers, 1992; Wallace, 1993). The Kayak disappears depositionally to the north in the Sadlerochit Mountains and exposures in the backlimb of the Sadlerochit Mountains anticlinorium indicate that the Shublik Mountains wedge cannot have penetrated that far northward (Fig. 4). Emplacement of such a wedge would account for northward tilt of strata in the south limb of the Ignek Valley syncline. The detailed geometry of this wedge would control whether it provided the amount and distribution of structural relief required to account fully for the fission-track data (Rogers, 1992; Wallace, 1993). Alternatively, the entire area that is now Ignek Valley syncline could have been uplifted above a detachment in the basement that lies below and forward of the Shublik Mountains horse.

Preferred Structural Model

The combination of structural observations and the fission-track data provide relatively strong restrictions on any interpretation of the structural evolution of the Sadlerochit Mountains and Ignek Valley. We constructed multiple structural cross sections to test whether a variety of structural interpretations were geometrically and kinematically viable and could account for the fission-track data. The structural geometry of the cross sections is generally consistent with the observed geometry, but was kept as simple as possible to facilitate testing multiple models. We used the same line of section as Cole et al. (1999) for several reasons. The line corresponds to the southern part of the Katakturuk River fission-track transect and is centrally located with respect to the Ignek Valley fission-track samples. The northern part of the line lies along seismic line 84–6 within the coastal plain of the Arctic National Wildlife Refuge (1002 area). Reprocessing of this seismic line provided the basis for the depth to the top of basement shown on the Cole et al. (1999) cross section. This is the most recently published depth interpretation and so was used as a starting point for defining the top of basement. Seismic line 84–6 has been published by Bruns et al. (1987, their Plate 4) and Potter et al. (1999, their Plate BD-2), which made it possible to assess variations in interpretation of the basement structure (Fig. 4B). Approximate stratigraphic thicknesses (Fig. 3) are based on thicknesses shown by Bird and Molenaar (1987, their Plate 1) from the Beli Unit #1 and Canning A-1 wells, ~25–30 km west of the line of section. Locations of faults and stratigraphic contacts and average dips are based on published maps and cross sections (Bader and Bird, 1986; Robinson et al., 1989; Wallace, 1993; Cole et al., 1999) and field observations.

We tested over a dozen different structural interpretations, each starting with the same restrictions derived from surface and subsurface data. Significant ''thin-skinned'' displacement and thickening have occurred above multiple detachments in the cover sequence. However, as explained previously, this deformation does not appear to account by itself either for the juxtaposition of the different age groups or the creation of sufficient structural relief to drive the requisite amount of erosional unroofing and cooling. Some amount of basement involvement seems necessary, so we assumed ''thick-skinned,'' basement-involved thrusting in all of our models. Structural geometry in the basement was delimited by the relief observed on the top of basement and the geometry of faults, which was based on surface observations and reflector geometry. A variety of basement-detachment configurations was tested—including different depths, flat versus dipping detachments, different depths in different parts of the section, and multiple levels of detachment. Different sequences of horse emplacement and breaching thrusts were tried to account for the distribution of fission-track ages.

The interpretation that most successfully accounts for the observed structures and the fission-track data is presented here (Fig. 14). An important element of this interpretation is the presence of two levels of structural detachment within the basement, at least southward from the Sadlerochit Mountains. This interpretation of the basement structure differs from most previously published interpretations for the area (e.g., Leiggi, 1987; Kelley and Foland, 1987; Cole et al., 1999), which identify only a single basement detachment. The double-detachment interpretation is not required by the fission-track data, but is based on structural observations and reasoning (Wallace, 1993). In the eastern Sadlerochit Mountains and western Shublik Mountains, the geometry of the anticlinoria suggests that nearly the entire thickness of each horse is exposed, supporting thickness estimates between ~2 and 4 km (Kelley and Foland, 1987; Leiggi, 1987; Meigs, 1989; Wallace, 1993; Cole et al., 1999) (Fig. 4). A similar horse thickness and an underlying subhorizontal detachment at a depth of ~4 km are supported by the apparently well-defined fault-bend-fold geometry observed farther south in the northeastern Brooks Range (Wallace, 1993). However, Wallace (1993) noted that a deeper detachment is required to account for the elevation of this shallow detachment and the overlying horses with respect to the ~5 km depth of the top of the basement beneath the coastal plain to the north (Fig. 14). Cole et al. (1999) proposed an alternative interpretation that relatively thin basement horses (~4 km) were elevated above a single detachment at a depth of ~8–9 km in the northeastern Brooks Range. However, we have not adopted this interpretation because it (1) requires greater displacement of basement horses than is compatible with the shortening observed in the immediately overlying cover, and (2) is inconsistent with the shallower subhorizontal detachment implied by the fault-bend-fold geometry of the basement anticlinoria (Wallace, 1993).

In our interpretation, the depth to the deeper detachment is based on the assumption that each in a series of down-to-the-north steps in the top of the basement beneath the coastal plain represents a horse formed above a common detachment depth (Fig. 14). This correspondence suggests a detachment at a depth slightly more than 9 km. The shallower detachment is slightly less than 3 km below the top of basement, according to the geometry of the Sadlerochit and Shublik Mountains horses. This position suggests that the shallower detachment is at a depth of slightly less than 4 km beneath the structural low in Ignek Valley.

The distribution and close juxtaposition of ca. 45 Ma and ca. 27 Ma fission-track ages north of the Sadlerochit Mountains range front are an important constraint on any structural interpretation (Fig. 14). Although the ca. 45 Ma apatite ages are found high in the stratigraphic section (Hue Shale or Canning Formation), the required relief is most readily explained by emplacement of basement horses. We interpret emplacement of two horses north of the Sadlerochit Mountains to account for the ca. 45 Ma ages that overlie them. The zircon ages along the range front of the Sadlerochit Mountains suggest that these rocks were elevated at the same time, but remained at greater depth than the

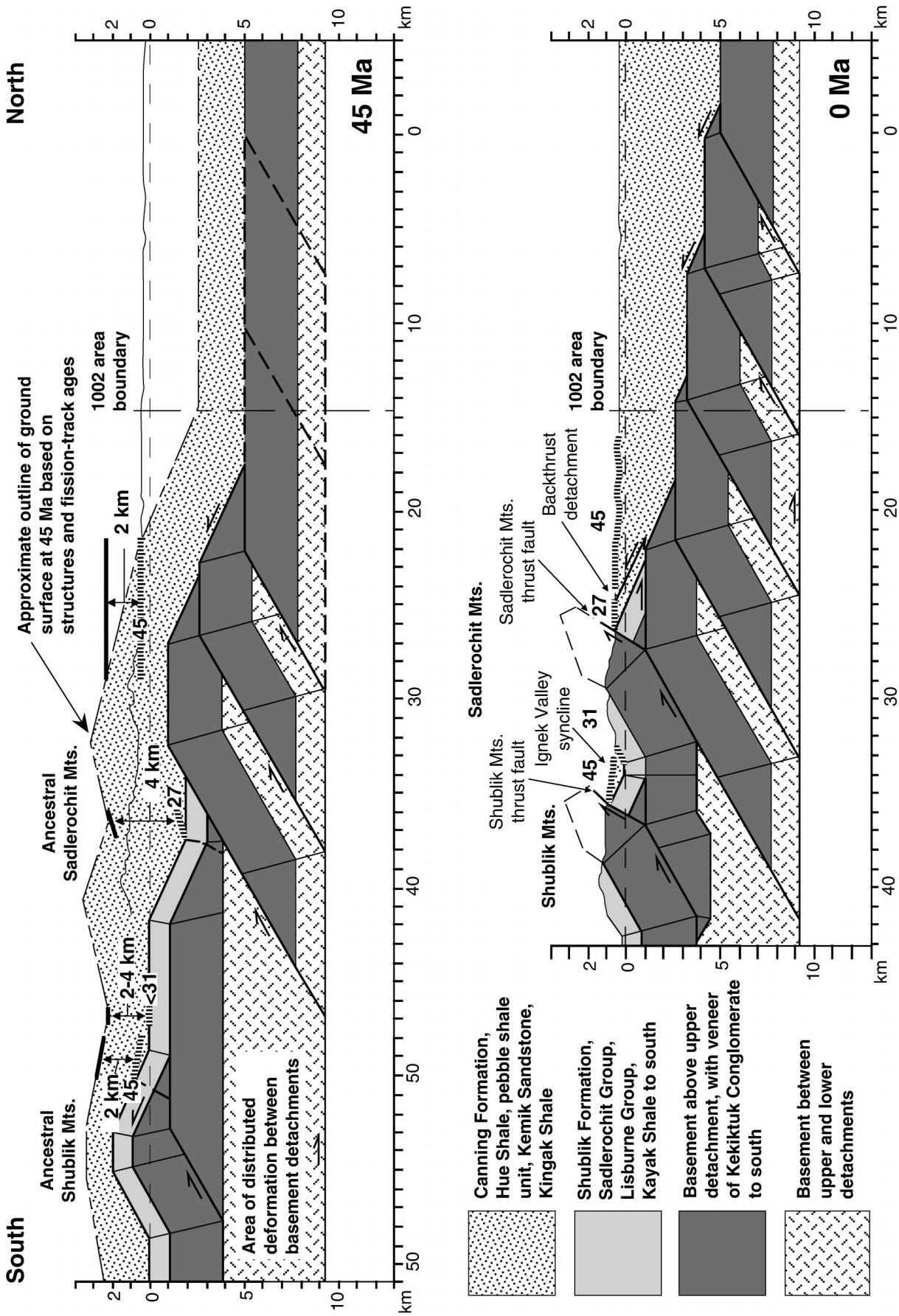

Figure 14. Simplified balanced cross section from Shublik Mountains to the Arctic coastal plain and a reconstruction to 45 Ma. Structure in Sadlerochit and Shublik Mountains based on surface data (Bader and Bird, 1986; Robinson et al., 1989; Wallace, 1993; Cole et al., 1999; field observations). Relief on basement beneath the coastal plain is based on seismic line 84–6 (Bruns et al., 1987; Potter et al., 1999). Vertical-stripe pattern indicates areas of fission-track data; adjacent numbers indicate time of cooling to ≤60 °C. On 45 Ma reconstruction, fission-track control on burial depths is specified numerically in kilometers and by heavy lines above data locations. Reconstructed paleotopography is based on burial depths inferred from thermochronologic data, but does not account for isostatic adjustment. "Area of distributed deformation between basement detachments" represents structural thickening by some combination of duplexing, folding, and penetrative strain; thickness between detachments does not represent thickness of an undeformed horse. See text for discussion of structures and their evolution.

horses to the north. Juxtaposition of the ca. 45 Ma and ca. 27 Ma apatite ages can be explained by emplacement at ca. 27 Ma of a basement wedge beneath a backthrust detachment. This wedge was emplaced from the south over the earlier-emplaced horses and thus is out of sequence with respect to the structurally underlying horses to the north. This wedge originally was the leading edge of the Sadlerochit Mountains horse on the basis of the geometry of its later, out of sequence truncation by the Sadlerochit Mountains thrust (Meigs, 1989; Wallace and Hanks, 1990; Wallace, 1993; Cole et al., 1999).

The fission-track data provide no direct indication of the age of emplacement of the two northernmost basement horses we interpret to underlie the coastal plain, but we infer them to have been emplaced during or shortly after the ca. 27 Ma event in the northern Sadlerochit Mountains. This inference is based on interpretation of seismic reflection data that suggests that the rocks overlying these horses were deformed in the late Oligocene to early Miocene (Potter et al., 1999). This deformation has been interpreted (Bruns et al., 1987; Kelley and Foland, 1987; Potter et al., 1999) to have resulted in formation of the Marsh Creek anticline (Figs. 2, 4B) as displacement of basement horses was accommodated in the cover by imbrication beneath a backthrust roof. The geometry of this structure is typical of a triangle zone (Jones, 1982, 1996) or passive-roof duplex (Banks and Warburton, 1986; Cooper, 1996). We infer that analogous triangle-zone structures formed at different locations in the cover, including above the leading edge of the Sadlerochit Mountains horse at ca. 27 Ma and above the two underlying horses at ca. 45 Ma.

A plausible structural interpretation to account for the fission-track data from Ignek Valley is more difficult to develop. Cooling in Ignek Valley at ca. 45 Ma can be most easily explained either by tilting above the leading edge of the Shublik Mountains horse or by uplift of the Ignek Valley syncline owing to thickening above a deep basement detachment (Fig. 14). Northward discontinuity of the Kayak Shale detachment limits how much uplift can be accommodated by emplacement of the Shublik Mountains wedge, probably to <2 km. Furthermore, this emplacement by itself probably could not account for the amount of relief interpreted to have been generated at the same time north of the Sadlerochit Mountains. Thus, it is unlikely that even 2 km of uplift along the northern edge of the Shublik Mountains horse could produce sufficient unroofing to account for the cooling ages in Ignek Valley. This conclusion suggests that uplift of the Ignek Valley syncline above a deep detachment likely played a significant role at ca. 45 Ma. The ca. 27 Ma apatite ages from the northern Sadlerochit Mountains place an important limitation on how such uplift could be accommodated. These ages suggest that these rocks remained buried at depths >4 km at the same time as stratigraphically equivalent rocks to the south in Ignek Valley were unroofed to just >2 km from the surface (Fig. 14). Thus, at ca. 45 Ma, the present Sadlerochit Mountains front would have been bounded by relative structural highs to the south and north. To account for this situation, we have hypothesized that thickening above a deeper detachment uplifted rocks south of the leading edge of the Sadlerochit Mountains horse and above the shallower basement detachment. This uplift may have occurred above a relatively flat-roofed duplex that formed between the two basement detachments. Little information is available to set limits on the original geometry of the roof of such a duplex, but the apparent displacement of the Sadlerochit Mountains horse on the upper basement detachment at ca. 27 Ma suggests that the detachment remained relatively flat. For simplicity, we have assumed uplift of the Ignek Valley syncline to its present elevation at ca. 45 Ma, although a lesser amount is possible. Displacement of the Sadlerochit Mountains horse on the upper basement detachment at ca. 27 Ma may have resulted in final cooling of apatites residing in the partial annealing zone in Ignek Valley.

We do not consider this interpretation to be either an exact or a unique solution. The focus of the model is on basement-involved structures, and it considers few structures in the cover. Large uncertainties exist on the depths inferred from the fission-track data, and these uncertainties allow considerable latitude in interpreting structural displacement. The actual structure is more complicated in detail, and it changes along strike. The fission-track data provide little control on paleotopography beyond what can be inferred from the interpreted burial depths relative to structure. Multiple structural possibilities exist at depth, despite the availability of some seismic reflection data.

Structural Implications

Despite the uncertainties in our structural interpretation, it illustrates some of the essential characteristics required for any structural interpretation to fit the fission-track data (Fig. 14). First, the amount of unroofing required to account for the fission-track ages suggests structural involvement of basement to create sufficient structural relief. Second, the distribution of ages suggests that activity of these basement-involved structures did not follow a simple forward-propagating sequence. Instead, the leading edge of activity apparently jumped significantly forward at ca. 45 Ma; then significant thickening occurred behind that point at ca. 27 Ma, and the leading edge of deformation moved incrementally forward at about the same time.

Although the sequence of basement-involved structures has not been addressed in detail in most previous interpretations of the area, a generally forward-propagating sequence has commonly been assumed (Kelley and Foland, 1987; O'Sullivan, 1993; O'Sullivan et al., 1993; Cole et al., 1999; Potter et al., 1999). Meigs (1989) and Rogers (1992) documented an out-of-sequence origin for the Sadlerochit and Shublik Mountains thrusts, respectively, and Mull (1987) showed that the Sadlerochit Mountains thrust cut across structures formed earlier in the cover. Cole et al. (1999) proposed a detailed sequence of basement activity that is forward propagating except for the late activity of these two thrusts. However, it is difficult to see how the distribution of ca. 45 and ca. 27 Ma fission-track ages can be accommodated without significant modification of both the structural geometry and sequence of their interpretation. Hanks et al. (1994) and O'Sullivan (1994) suggested out-of-sequence activity in the Sadlerochit and Shublik Mountains, but they did not relate activity at specific times to specific structures as we have done here. Moore (1999) used seismic reflection data and fission-track data to identify out-of-sequence activity of basement horses in the subsurface of the coastal plain east of the Sadlerochit Mountains. He documented that probable Miocene emplacement of horses, including the eastern correlative of the Sadlerochit Mountains horse, was preceded by late Eocene emplacement of a horse farther to the north. Although the geometry and timing may differ in detail, our results independently confirm out-of-sequence activity of basement horses near the range front of the northeastern Brooks Range.

The results of this study have a number of broader tectonic implications. First, it documents that tectonic activity occurred at ca. 45 and ca. 27 Ma >1200 km landward of the present convergent boundary between the Pacific and North American plates. The explanation for deformation so far within the continent at this time is uncertain. Widespread arc magmatism in southwestern Alaska is interpreted to have been the result of a gently dipping subduction zone (Wallace and Eng-

ebretson, 1984; Moll-Stalcup, 1994), as has been hypothesized for the origin of the Laramide Rockies far within the continent. However, this period of gently dipping subduction was at an earlier time (ca. 74–56 Ma). The earlier period of deformation within the Sadlerochit Mountains coincides with a period of plate reorganization (ca. 56–43 Ma) associated with the demise of the Kula plate (e.g., Lonsdale, 1988). A higher rate and more northward direction of convergence during at least part of this time resulted in considerable strike-slip faulting throughout Alaska, combined with counterclockwise rotation in western Alaska (e.g., Wallace and Engebretson, 1984; Plafker and Berg, 1994; Moore et al., 1994b). The indentation of Alaska that resulted at the hinge of this bend could help account for deformation in the northeastern Brooks Range at ca. 45 Ma. After ca. 43 Ma, convergence slowed and was more toward the northwest. Rotation of western Alaska and indentation at the hinge has continued to the present, although at a significantly decreased rate (e.g., Plafker and Berg, 1994; Moore et al., 1994b). Deformation in the northeastern Brooks Range at ca. 27 Ma may have resulted from this continued indentation, although no other major tectonic ''event'' elsewhere in Alaska obviously coincides with this time.

Both periods of far intracontinental deformation in northeastern Alaska involved basement. Depth to basement in the foreland of the evolving Brooks Range decreased northward toward the Barrow arch, a long-standing subsurface structural high near the present Arctic coastline (e.g., Moore et al., 1994a). As the deforming wedge of the northeastern Brooks Range grew northward, it moved up the gently south-dipping basement surface and incorporated the upper part of the basement as it went. The out-of-sequence deformation within the basement is consistent with the predictions of critical-wedge models for fold-and-thrust belts (e.g., Dahlen, 1990; Hardy et al., 1998). Out-of-sequence deformation may reflect internal thickening of the wedge at ca. 27 Ma that allowed it to reattain critical taper following erosion that resulted from the ca. 45 Ma deformation.

Implications for Hydrocarbons

The preferred thermal and structural model for the Sadlerochit Mountains region has profound implications for the generation and preservation of hydrocarbons within the region and in the coastal plain immediately to the north of the mountain front. The model suggests that (1) for the rocks sampled, maximum paleotemperatures and therefore peak hydrocarbon generation from potential hydrocarbon source rocks occurred during the early to middle Cenozoic, and (2) deformation within the Sadlerochit Mountains and to the immediate north occurred since middle Eocene time. Therefore, peak hydrocarbon generation in the Sadlerochit Mountains vicinity predated formation of potential trapping structures, so that any hydrocarbons generated from the region would have probably migrated through the system. However, hydrocarbons generated from these rocks could potentially have migrated updip into existing stratigraphic traps prior to structural deformation. Furthermore, hydrocarbons generated later in more distal parts of the basin could have migrated updip into subsurface structures formed in middle Eocene and late Oligocene time north of the Sadlerochit Mountains and along strike to the east and west.

CONCLUSIONS

Fission-track data from this study document two periods of rapid cooling at 45 ± 3 Ma (middle Eocene) and 27 ± 2 Ma (late Oligocene). These cooling events are interpreted to reflect erosional denudation resulting from uplift due to structural thickening. Detailed fission-track data from the Sadlerochit Mountains and Ignek Valley set limits on the time, rate, and amount of denudation associated with each of these deformational episodes. The results suggest that prior to middle Eocene denudation, rocks currently exposed at the surface were between ~4 and 8 km below the surface. Rocks both north and south of the Sadlerochit Mountains underwent at least 2 km of denudation in response to uplift during the middle Eocene. At least 2 km of denudation occurred in response to uplift immediately north of the Sadlerochit Mountains during the late Oligocene, and some uplift and denudation probably occurred at the same time in and south of the Sadlerochit Mountains. Deformation was episodic, with significant structural thickening occurring in a relatively short (~5 m.y.) period of time.

The distribution of ages with respect to structural detachments and structurally thickened sections supports involvement of basement in structures associated with both cooling events. At least one basement horse probably was emplaced at ca. 45 Ma north of the Sadlerochit Mountains. The Sadlerochit Mountains horse was probably emplaced out of sequence at ca. 27 Ma behind the earlier-emplaced horse(s), at about the same time as basement-involved deformation beneath the coastal plain to the north led to formation of the Marsh Creek anticline in the cover. Both deformational events represent intracontinental deformation that occurred >1200 km from the southern Alaska convergent plate boundary, perhaps due to indentation of southern Alaska.

The fission-track data suggest that maximum paleotemperatures, and hence peak hydrocarbon generation, predated formation of potential trapping structures during middle Eocene deformation in the Sadlerochit Mountains vicinity. However, hydrocarbons generated in more distal parts of the basin that reached maximum burial at a later time could have migrated updip into subsurface structures formed in middle Eocene and late Oligocene time north of the Sadlerochit Mountains and along strike to the east and west.

ACKNOWLEDGMENTS

This work was made possible by funding from the industry sponsors of the Tectonics and Sedimentation Research Group at the University of Alaska Fairbanks; the donors of the Petroleum Research Fund, distributed by the American Chemical Society (no. 24101-AC2); Geotrack International Pty. Ltd.; and the U.S. Minerals Management Service Continental Margins Project (Cooperative Agreement no. 14-12-0001-30432). Support for the sample irradiations at the HIFAR reactor at Lucas Heights, Australia, was supplied either through an Australian Institute of Nuclear Science and Engineering grant or by Geotrack International Pty. Ltd. The State of Alaska Division of Geological and Geophysical Surveys and the Tectonics and Sedimentation Research Group provided field and logistical support. The manuscript has been greatly improved on the basis of reviews by Gil Mull, Raymond Donelick, and Paul Mann.

REFERENCES CITED

ANWR Assessment Team, 1999, Oil and gas resource potential of the 1002 area, Arctic National Wildlife Refuge, Alaska: U.S. Geological Survey Open-File Report 98–34, CD-ROM (see also individual parts cited herein).

Bader, J.W., and Bird, K.J., 1986, Geologic map of the Demarcation Point, Mount Michelson, Flaxman Island, and Barter Island quadrangles, Alaska: U.S. Geological Survey Miscellaneous Investigations Map I-1791, 1 sheet, scale 1:250,000.

Banks, C.J., and Warburton, J., 1986, ''Passive-roof'' duplex geometry in the frontal structures of the Kirthar and Sulaiman mountain belts, Pakistan: Journal of Structural Geology, v. 8, p. 229–237.

Bird, K.J., and Magoon, L.B., eds., 1987, Petroleum geology of the northern part of the Arctic National Wildlife Refuge, northeastern Alaska: U.S. Geological Survey Bulletin 1778, 329 p.

Bird, K.J., and Molenaar, C.M., 1987, Stratigraphy, *in* Bird, K.J., and Magoon, L.B., eds.,

Petroleum geology of the northern part of the Arctic National Wildlife Refuge, northeastern Alaska: U.S. Geological Survey Bulletin 1778, p. 37–59.

Blythe, A.E., Bird, J.M., and Omar, G.I., 1996, Deformational history of the central Brooks Range, Alaska: Results from fission-track and $^{40}Ar/^{39}Ar$ analyses: Tectonics, v. 15, p. 440–455.

Boyer, S.E., and Elliot, D., 1982, Thrust sytems: American Association of Petroleum Geologists Bulletin, v. 66, p. 1196–1230.

Brandon, M.T., Roden-Tice, M.K., and Garver, J.I., 1998, Late Cenozoic exhumation of the Cascadia accretionary wedge in the Olympic Mountains, northwest Washington State: Geological Society of America Bulletin, v. 110, p. 985–1009.

Bruns, T.R., Fisher, M.A., Leinbach, W.J., Jr., and Miller, J.J., 1987, Regional structure of rocks beneath the coastal plain, *in* Bird, K.J., and Magoon, L.B., eds., Petroleum geology of the northern part of the Arctic National Wildlife Refuge, northeastern Alaska: U.S. Geological Survey Bulletin 1778, p. 249–254.

Burnham, A.K., and Sweeney, J.J., 1989, A chemical kinetic model of vitrinite maturation and reflectance: Geochimica et Cosmochimica Acta, v. 53, p. 2649–2657.

Butler, R.W.H., 1987, Thrust sequences: Journal of the Geological Society of London, v. 144, p. 619–634.

Carlson, W.D., Donelick, R.A., and Ketcham, R.A., 1999, Variability of apatite fission-track annealing kinetics: I. Experimental results: American Mineralogist, v. 84, p. 1213–1223.

Carter, L.D., Ferrians, O.J., Jr., and Galloway, J.P., 1986, Engineering-geologic maps of northern Alaska, coastal plain and foothills of the Arctic National Wildlife Refuge: U.S. Geological Survey Open-File Report 86–334, scale 1:250,000.

Cole, F., Bird, K.J., Mull, C.G., Wallace, W.K., Sassi, W., Murphy, J.M., and Lee, M., 1999, A balanced cross section and kinematic and thermal model across the northeastern Brooks Range mountain front, Arctic National Wildlife Refuge, Alaska, *in* ANWR Assessment Team, Oil and gas resource potential of the 1002 area, Arctic National Wildlife Refuge, Alaska: U.S. Geological Survey Open-File Report 98–34, CD-ROM, p. SM 1–60.

Cooper, M., 1996, Passive-roof duplexes and pseudopassive-roof duplexes at mountain fronts: A review: Bulletin of Canadian Petroleum Geology, v. 44, p. 410–421.

Dahlen, F.A., 1990, Critical taper model of fold-and-thrust belts and accretionary wedges: Annual Review of Earth and Planetary Sciences, v. 18, p. 55–99.

Dixon, J., and Dietrich, J.R., 1990, Canadian Beaufort Sea and adjacent land areas, *in* Grantz, A., Johnson, L., and Sweeney, J.F., eds., The Arctic Ocean region: Boulder, Colorado, Geological Society of America, Geology of North America, v. L, p. 239–256.

Donelick, R.A., Ketcham, R.A., and Carlson, W.D., 1999, Variability of apatite fission-track annealing kinetics: II. Crystallographic orientation effects: American Mineralogist, v. 84, p. 1224–1234.

England, P., and Molnar, P., 1990, Surface uplift, uplift of rocks, and exhumation of rocks: Geology, v. 18, p. 1173–1177.

Erslev, E.A., 1986, Basement balancing of Rocky Mountain foreland uplifts: Geology, v. 14, p. 259–262.

Fitzgerald, P.G., and Gleadow, A.J.W., 1988, Fission track geochronology, tectonics and structure of the Transantarctic Mountains in northern Victoria Land, Antarctica: Chemical Geology (Isotope Geoscience Section), v. 73, p. 169–198.

Gleadow, A.J.W., Duddy, I.R., Green, P.F., and Lovering J.F., 1986, Confined fission track lengths in apatite: A diagnostic tool for thermal history analysis: Contributions to Mineralogy and Petrology, v. 94, p. 405–415.

Grantz, A., Dinter, D.A., and Culotta, R.C., 1987, Structure of the continental shelf north of the Arctic National Wildlife Refuge, *in* Bird, K.J., and Magoon, L.B., eds., 1987, Petroleum geology of the northern part of the Arctic National Wildlife Refuge, northeastern Alaska: U.S. Geological Survey Bulletin 1778, p. 271–276.

Green, P.F., Duddy, I.R., Gleadow, A.J.W., Tingate, P.T., and Laslett, G.M., 1985, Fission track annealing in apatite: Track length measurements and the form of the Arrhenius plot: Nuclear Tracks, v. 10, p. 323–328.

Green, P.F., Duddy, I.R., Gleadow, A.J.W., and Lovering, J.F., 1989, Apatite fission track analysis as a paleotemperature indicator for hydrocarbon exploration, *in* Naeser, N.D., ed., Thermal history of sedimentary basins—Methods and case histories: New York, Springer-Verlag, p. 181–195.

Grow, J.A., Potter, C.J., Perry, W.J., Jr., Lee, M.W., and Killgore, M., 1999, Structural framework and lithologic composition of the Niguanak high and the Aurora dome, *in* ANWR Assessment Team, Oil and Gas Resource Potential of the 1002 area, Arctic National Wildlife Refuge, Alaska: U.S. Geological Survey Open-File Report 98-34, CD-ROM, p. NA 1–46.

Hanks, C.L., Wallace, W.K., and O'Sullivan, P., 1994, The Cenozoic structural evolution of the northeastern Brooks Range, Alaska, *in* Thurston, D., and Fujita, K., eds., 1992 Proceedings, International Conference on Arctic Margins: U.S. Minerals Management Service Outer Continental Shelf Study 94–0040, p. 263–268.

Hardy, S., Duncan, C., Masek, J., and Brown, D., 1998, Minimum work, fault activity, and the growth of critical wedges in fold and thrust belts: Basin Research, v. 10, p. 365–373.

Jones, P.B., 1982, Oil and gas beneath east-dipping underthrust faults in the Alberta foothills, *in* Powers, R.B., ed., Geological studies of the Cordilleran thrust belt, Volume 1: Denver, Colorado, Rocky Mountain Association of Geologists, p. 61–74.

Jones, P.B., 1996, Triangle zone geometry, terminology and kinematics: Bulletin of Canadian Petroleum Geology, v. 44, p. 139–152.

Kelley, J.S., and Foland, R.L., 1987, Structural style and framework geology of the coastal plain and adjacent Brooks Range, *in* Bird, K.J., and Magoon, L.B., eds., Petroleum geology of the northern part of the Arctic National Wildlife Refuge, northeastern Alaska: U.S. Geological Survey Bulletin 1778, p. 255–270.

Ketcham, R.A., Carlson, W.D., and Donelick, R.A., 1999, Variability of apatite fission-track annealing kinetics: III. Extrapolation to geologic timescales: American Mineralogist, v. 84, p. 1235–1255.

Laslett, G.M., Green, P.F., Duddy, I.R., and Gleadow, A.J.W., 1987, Thermal modelling of fission tracks in apatite: 2. A quantitative analysis: Chemical Geology, v. 65, p. 1–13.

Leiggi, P.A., 1987, Style and age of tectonism of the Sadlerochit Mountains to Franklin Mountains, Arctic National Wildlife Refuge, Alaska, *in* Tailleur, I.L., and Weimer, P., eds., Alaskan North Slope geology: Pacific Section, SEPM (Society of Economic Paleontologists and Mineralogists) and Alaska Geological Society, Book 50, p. 749–756.

Lonsdale, P., 1988, Paleogene history of the Kula plate: Offshore evidence and onshore implications: Geological Society of America Bulletin, v. 100, p. 733–754.

Magoon, L.B., Woodward, P.V., Banet Jr., A.C., Griscom, S.B., and Daws, T.A., 1987, Thermal maturity, richness, and type of organic matter of source-rocks units, *in* Bird, K.J., and Magoon, L.B., eds., Petroleum geology of the northern part of the Arctic National Wildlife Refuge, northeastern Alaska: U.S. Geological Survey Bulletin 1778, p. 127–180.

McMillen, K.J., and O'Sullivan, P.B., 1992, Tectonic and eustatic controls on Paleogene sequence stratigraphy: Beaufort Sea, Alaska and Canada, *in* Watkins, J.S., Zhiqiang, F., and McMillen, K.J., eds., Geology and geophysics of continental margins: American Association of Petroleum Geologists Memoir 53, p. 285–301.

Meigs, A.J., 1989, Structural geometry and sequence in the eastern Sadlerochit Mountains, northeastern Brooks Range, Alaska [M.S. thesis]: Fairbanks, University of Alaska, 220 p.

Mitra, S., and Mount, V.S., 1998, Foreland basement structures: American Association of Petroleum Geologists Bulletin, v. 82, p. 70–109.

Moll-Stalcup, E.J., 1994, Latest Cretaceous and Cenozoic magmatism in mainland Alaska, *in* Plafker, G., and Berg, H.C., eds., The geology of Alaska: Boulder, Colorado, Geological Society of America, Geology of North America, v. G-1, p. 589–619.

Moore, T.E., 1999, Balanced cross section, Bathtub syncline to Beaufort Sea through Niguanank structural high, Arctic National Wildlife Refuge (ANWR), northeastern Alaska, *in* ANWR Assessment Team, Oil and gas resource potential of the 1002 area, Arctic National Wildlife Refuge, Alaska: U.S. Geological Survey Open-File Report 98–34, CD-ROM, p. BC 1–61.

Moore, T.E., Wallace, W.K., Bird, K.J., Karl, S.M., Mull, C.G., and Dillon, J.T., 1994a, Geology of northern Alaska, *in* Plafker, G., and Berg, H., eds., The geology of Alaska: Boulder, Colorado, Geological Society of America, Geology of North America, v. G1, Chapter 3.

Moore, T.E., Grantz, A., and Roeske, S.M., 1994b, Continent-ocean transition in Alaska: The tectonic assembly of eastern Denalia, *in* Speed, R.C., ed., Phanerozoic evolution of North American continent-ocean transitions: Boulder, Colorado, Geological Society of America, DNAG Continent-Ocean Transect Volume, p. 399–441.

Morley, C.K., 1988, Out-of-sequence thrusts, Tectonics, v. 7, p. 539–561.

Mull, C.G., 1982, Tectonic evolution and structural style of the Brooks Range, Alaska: An illustrated summary, *in* Powers, R.B., ed., Geological studies of the Cordilleran thrust belt, Volume 1: Denver, Colorado, Rocky Mountain Association of Geologists, p. 1–45.

Mull, C.G., 1987, Kemik Sandstone, Arctic National Wildlife Refuge, northeastern Alaska, *in* Tailleur, I.L., and Weimer, P., eds., Alaskan North Slope geology: Pacific Section SEPM and Alaska Geological Society, book 50, p. 405–431.

Naeser, C.W., 1979, Fission track dating and geologic annealing of fission tracks, *in* Jager, E., and Hunziker, J.C., eds., Lectures in isotope geology: New York, Springer-Verlag, p. 154–169.

O'Sullivan, P.B., 1993, Late Cretaceous and Tertiary thermal and uplift history of the North Slope foreland basin of northern Alaska and northwestern Canada [Ph.D. thesis]: Bundoora, Victoria, Australia, La Trobe University, 419 p.

O'Sullivan, P.B., 1994, Timing of Tertiary episodes of uplift and erosion, northeastern Brooks Range, Alaska, *in* Thurston, D., and Fujita, K., eds., 1992 Proceedings, International Conference on Arctic Margins: U.S. Minerals Management Service Outer Continental Shelf Study 94–0040, p. 269–274.

O'Sullivan, P.B., 1996, Late Mesozoic and Cenozoic thermal-tectonic evolution of the North Slope foreland basin, Alaska, *in* Johnsson, M.J., and Howell, D.G., eds., Thermal evolution of sedimentary basins in Alaska: U.S. Geological Survey Bulletin 2142, p. 45–79.

O'Sullivan, P.B., 1999, Thermochronology, denudation, and variations in paleosurface temperature: A case study from the North Slope foreland basin, Alaska: Basin Research, v. 11, no. 3, p. 191–205.

O'Sullivan, P.B., and Brown, R.W., 1998, Effects of surface cooling on apatite fission track data: Evidence for Miocene climatic change, North Slope, Alaska, *in* Van den Haute, P., and De Corte, F., eds., Advances in fission track geochronology: Dordrecht, Netherlands, Kluwer Academic Publishers, p. 255–267.

O'Sullivan, P.B., Green, P.F., Bergman, S.C., Decker, J., Duddy, I.R., Gleadow, A.J.W., and Turner, D.L., 1993, Multiple phases of Tertiary uplift and erosion in the Arctic National Wildlife Refuge, Alaska, revealed by apatite fission track analysis: American Association of Petroleum Geologists Bulletin, v. 77, p. 359–385.

O'Sullivan, P.B., Murphy, J.M., and Blythe, A.E., 1997, Late Mesozoic and Cenozoic thermotectonic evolution of the Central Brooks Range and adjacent North Slope foreland basin, Alaska: Including fission track results from the Trans-Alaska Crustal Transect (TACT): Journal of Geophysical Research, v. 102, p. 20,821–20,845.

O'Sullivan, P.B., Moore, T.E., and Murphy, J.M., 1998a, Tertiary uplift of the Mount Doonerak antiform, central Brooks Range, Alaska: Apatite fission track evidence from the Trans-Alaska Crustal Transect, *in* Oldow, J., and Avé Lallement, H., eds., Architecture of the Central Brooks Range fold and thrust belt, Arctic Alaska: Geological Society of America Special Paper 324, p. 245–259.

O'Sullivan, P.B., Wallace, W.K., and Murphy, J.M., 1998b, Fission track evidence for apparent out-of-sequence Cenozoic deformation along the Philip Smith Mountain front, northeastern Brooks Range, Alaska: Earth and Planetary Science Letters, v. 164, no. 3–4, p. 435–449.

Plafker, G., and Berg, H.C., 1994, Overview of the geology and tectonic evolution of Alaska, *in* Plafker, G., and Berg, H.C., eds., The geology of Alaska: Boulder, Colorado, Geological Society of America, Geology of North America, v. G-1, p. 989–1021.

Potter, C.J., Perry, W.J., Grow, J.A., and Lee, M.W., 1999, Style and timing of thrust-faulting in the 1002 area, Arctic National Wildlife Refuge, *in* ANWR Assessment Team, Oil and gas resource potential of the 1002 area, Arctic National Wildlife Refuge, Alaska: U.S. Geological Survey Open-File Report 98–34, CD-ROM, p. BD 1–32.

Reiser, H.N., Dutro, J.T., Jr., Brosgé, W.P., Armstrong, A.K., and Detterman, R.L., 1970, Progress map, geology of the Sadlerochit and Shublik Mountains, Mount Michelson C-1, C-2, C-3, and C-4 quadrangles, Alaska: U.S. Geological Survey Open-File Report 70–273, scale 1:63,360, 5 sheets.

Reiser, H.N., Brosgé, W.P., Dutro, J.T., Jr., and Detterman, R.L., 1971, Preliminary geologic map, Mount Michelson quadrangle, Alaska: U.S. Geological Survey Open-File Report 71–237, 5 sheets, scale 1:200,000, 2 sheets.

Robinson, M.S., Decker, J., Clough, J.G., Reifenstuhl, R.R., Bakke, A., Dillon, J.T., Combellick, R.A., and Rawlinson, S.A., 1989, Geology of the Sadlerochit and Shublik Mountains, Arctic National Wildlife Refuge, northeastern Alaska: Alaska Division of Geological and Geophysical Surveys Professional Report 100, scale 1:63,360, 1 sheet.

Rogers, J.A., 1992, Lateral variation of range-front structures and structural evolution of the central Shublik Mountains and Ignek Valley, northeastern Brooks Range, Alaska [M.S. thesis]: Fairbanks, University of Alaska, 128 p.

Rowan, E.L., 1999, Timing and extent of oil generation, Canning River region, North Slope, Alaska, based on a reconstruction of burial and conductive heat flow history, *in* ANWR Assessment Team, Oil and gas resource potential of the 1002 area, Arctic National Wildlife Refuge, Alaska: U.S. Geological Survey Open-File Report 98–34, CD-ROM, p. BE-1–59.

Tagami, T., Ito, H., and Nishimura, S., 1990, Thermal annealing characteristics of spontaneous fission tracks in zircon: Chemical Geology, v. 80, p. 159–169.

Wallace, W.K., 1993, Detachment folds and a passive-roof duplex: Examples from the northeastern Brooks Range, Alaska, *in* Solie, D.N., and Tannian, F., eds., Short notes on Alaskan geology 1993: Alaska Division of Geological and Geophysical Surveys Geologic Report 113, p. 81–99.

Wallace, W.K., and Engebretson, D.C., 1984, Relationships between plate motions and Late Cretaceous to Paleogene magmatism in southwestern Alaska: Tectonics, v. 3, p. 295–315; Publisher's correction: Tectonics, v. 3, p. 497–498.

Wallace, W.K., and Hanks, C.L., 1990, Structural provinces of the northeastern Brooks Range, Arctic National Wildlife Refuge, Alaska: American Association of Petroleum Geologists Bulletin, v. 74, p. 1100–1118.

Manuscript Received by the Society 18 June 2001
Revised Manuscript Received 4 April 2002
Manuscript Accepted 2 May 2002

Printed in the USA